Variability in flood frequency in sub-Saharan Africa: The role of large-scale climate modes of variability and their future impacts

Job Ekolu, Bastien Dieppois, Yves Tramblay, Gabriele Villarini, Louise J Slater, Gil Mahé, Jean-Emmanuel Paturel, Jonathan M Eden, Simon Moulds, Moussa Sidibe, et al.

Journal of Hydrology 640 (2024) 131679

Contents lists available at ScienceDirect

Journal of Hydrology

journal homepage: www.elsevier.com/locate/jhydrol

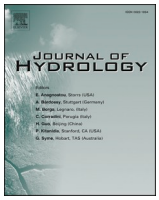

Research papers

Variability in flood frequency in sub-Saharan Africa: The role of large-scale climate modes of variability and their future impacts

Job Ekolu [a,*], Bastien Dieppois [a], Yves Tramblay [b], Gabriele Villarini [c], Louise J. Slater [d], Gil Mahé [e], Jean-Emmanuel Paturel [e], Jonathan M. Eden [a], Simon Moulds [f], Moussa Sidibe [g], Pierre Camberlin [h], Benjamin Pohl [h], Marco van de Wiel [a,i]

[a] Centre for Agroecology, Water and Resilience (CAWR), Coventry University, Coventry, UK
[b] Espace-Dev, Univ. Montpellier, IRD, Montpellier, France
[c] Department of Civil and Environmental Engineering and High Meadows Environmental Institute, Princeton University, Princeton, NJ, USA
[d] School of Geography and the Environment, University of Oxford, Oxford, UK
[e] HSM, Univ. Montpellier, CNRS, IRD, Montpellier, France
[f] School of GeoSciences, University of Edinburgh, UK
[g] Global Facility for Disaster Reduction and Recovery (GFDRR), World Bank, Washington DC, USA
[h] Centre de Recherches de Climatologie, UMR 6282 Biogéosciences CNRS/Université de Bourgogne Franche-Comté, Dijon, France
[i] College of Agriculture and Environmental Sciences, UNISA, FL, South Africa

ARTICLE INFO

This manuscript was handled by Andras Bardossy, Editor-in-Chief, with the assistance of Ashish Sharma, Associate Editor

Keywords:
Flood Frequency
Internal Climate variability
Sub-Saharan Africa
CMIP5/6 Single Model Initial Condition Large Ensembles (SMILEs)
Observed and Future Impacts

ABSTRACT

Sub-Saharan Africa (SSA) is strongly affected by flood hazards, endangering human lives and economic stability. However, the role of internal climate modes of variability in driving fluctuations in SSA flood occurrence remains poorly documented and understood. To address this gap, we quantify the relative and combined contribution of large-scale climate drivers to seasonal and regional flood occurrence using a new 65-year daily streamflow dataset, sea-surface temperatures derived from observations, and 12 Single Model Initial-condition Large Ensembles (SMILEs) from the Coupled Model Intercomparison Project Phases 5 and 6. We find significant relationships between floods and large-scale climate variability across SSA, with climatic drivers accounting for 30–90 % of the variability in floods. Notably, western, central, and the summer-rain region of southern Africa display stronger teleconnections to large-scale climate variability in comparison to East Africa and the winter-rain region of South Africa, where regional circulation patterns and human activities may play a more important role. In southern and eastern Africa, floods are mainly influenced by teleconnections with the Pacific and Indian Oceans, while in western and central Africa, teleconnections with the Atlantic Ocean and Mediterranean Sea play a larger role. We also find that the number of floods is projected to fluctuate by ± 10–50 % during the 21st century in response to different sequences of key modes of climate variability. We also note that the relative contributions of large-scale climate variability to future flood risks are generally consistent across all SMILEs. Our findings thus provide valuable information for long-term disaster risk reduction and management.

1. Introduction

State-of-the-art climate change projections suggest a potential increase in the frequency and intensity of flooding for several regions across the world (*e.g.,* Gosling & Arnell, 2016; Winsemius et al., 2016) but large uncertainties remain (*e.g.,* Kundzewicz et al., 2019). To develop more robust risk prediction and sustainable management strategies, there is a need to better understand the drivers of regional flood characteristics, as well as their impact on future change. This is notably important in vulnerable regions, such as Sub-Saharan Africa (SSA; *e.g.,* Niang et al., 2014; Shiferaw et al., 2014), where floods result in loss of lives, infrastructure damage, and economic losses (Bates et al., 2008).

Many parts of SSA are poorly represented in global climate and hydrological datasets (Mahe et al., 2013; Nobre et al., 2017; Tramblay et al., 2020a; Harrigan et al., 2020; Dixon et al., 2022). Existing studies are often restricted to the catchment scale (*e.g.,* Valimba et al., 2005;

* Corresponding author at: Job Ekolu, Centre for Agroecology, Water and Resilience (CAWR), Coventry University, Ryton Gardens, Ryton on Dunsmore, Coventry, CV8 3LG, UK.
E-mail address: ekoluj@uni.coventry.ac.uk (J. Ekolu).

https://doi.org/10.1016/j.jhydrol.2024.131679
Received 8 November 2023; Received in revised form 27 June 2024; Accepted 1 July 2024
Available online 14 July 2024

Conway et al., 2009; Taye and Willems, 2012; Nyeko-Ogiramoi et al., 2013; Chun et al., 2021), limiting our interpretation of the relative influence of climate change and variability on hydrological trends from that of catchment properties (*e.g.,* groundwater interactions, land-use/land cover change, and water management activities; Kingston et al. 2020). In recent years, the barriers to progress have been reduced through efforts aimed at compiling hydrological datasets from diverse sources (Tramblay et al., 2020a) and creating a complete daily streamflow dataset for SSA (Ekolu et al., 2022).

Existing studies have consistently reported increasing trends in flood magnitude witnessed during the 20th and early 21st centuries over western Africa (Descroix et al., 2013, 2018; Nka et al., 2015; Aich et al., 2016; Andersson et al., 2017; Wilcox et al., 2018; Tramblay et al., 2020b; Rameshwaran et al., 2021; Dembélé et al., 2022; Ekolu et al., 2022), eastern Africa (Taye et al., 2015; Taye & Willems, 2012; Bernard et al., 2013; Degefu et al., 2019; Tramblay et al., 2020b; Ekolu et al., 2022), and southern Africa (Do et al., 2017; Tramblay et al., 2020b; Ekolu et al., 2022; Franchi et al., 2024). However, as pointed out in Ekolu et al. (2022), observed trends in the frequency, intensity, and duration of floods across all SSA regions show significant interannual to decadal variability, with poorly understood driving factors. Ficchì et al. (2021) reported a high spatial dispersion and low signal-to-noise ratio in the relationship between flood magnitudes and different modes of climate variability, but this study relied on the short duration (*i.e.,* 35 years) and low quality GloFas-ERA-Interim/Land streamflow reanalysis over Africa (Harrigan et al. 2020). Nevertheless, identifying the large-scale drivers of those variations in flood characteristics is crucial to develop more reliable and seamless (seasonal-to-decadal) flood forecasting systems. For instance, empirical seasonal forecasts of historical flood probabilities based on El Niño Southern Oscillation (ENSO) have been shown to outperform dynamical modelling approaches in many parts of Africa (Emerton et al., 2019). In addition, there are many other modes of climate variability that emerge as important and predictable independent drivers of climate and hydrological variability across SSA. While ENSO is the leading mode of climate variability affecting rainfall variability in SSA on interannual timescales (*e.g.,* Reason et al., 2000; Giannini et al., 2005, 2008; Rodríguez-Fonseca et al., 2015; Parhi et al., 2016), other studies highlighted significant influences of sea-surface temperature anomalies (SSTa) over the Tropical North and South Atlantic (*e.g.,* Camberlin and Okoola, 2003; Losada et al., 2010; Williams et al., 2012), the Mediterranean Sea (*e.g.,* Rowell, 2013; Fontaine et al., 2010; Gaetani et al., 2010), and the Indian Ocean (*e.g.,* Saji et al., 1999; Webster et al., 1999; Black et al., 2003; Manatsa et al., 2012; Manatsa and Behera 2013). Similarly, the Atlantic Multidecadal Variability (AMV) and other decadal climate variations in the Pacific and Indian Oceans were found to play a substantial role in modulating rainfall in SSA on decadal timescales (*e.g.*, Biasutti et al., 2008; Mohino et al., 2011; Dieppois et al., 2013, 2016, 2019). Some studies also suggested that interannual to decadal changes in streamflow and flood magnitude could be linked to variations in SSTa (*e.g.*, Taye & Willems, 2012; Bernard et al., 2013; Sidibe et al., 2019; Kundzewicz et al., 2019; Tramblay et al., 2020b; Franchi et al., 2024). How these different modes of climate variability interact with each other and affect flood characteristics is, however, less understood (Kundzewicz et al., 2019). To address these shortcomings, our study takes advantage of a newly developed observation-based 65-year long daily streamflow datasets, covering all SSA, to examine the relative importance of each mode of climate variability on the occurrence of flood hazards across SSA.

Furthermore, as illustrated in various papers focusing on North America (Deser et al., 2012, 2014, 2016), Europe (Maher et al., 2021; Deser et al., 2023), and West Africa (Monerie et al., 2017), internal climate modes of variability, such as ENSO and AMV, are likely to enhance or dampen the impact of anthropogenic climate change from one decade to another at the regional scale over the 21st century. Yet, most existing projections of flood risk typically employ single simulations of global/regional climate models, which does not enable scientists and stakeholders to quantify and separate the impacts of internal climate variability and externally forced, *i.e.,* anthropogenic, climate changes (*e.g.,* Maher et al., 2021; Deser and Phillips, 2023). Most climate change impact studies also typically used bias-correction approaches, which are based on the evaluation of a single simulation from one or multiple climate models (*e.g.,* Hirabayashi et al., 2013; Dankers et al., 2014), neglecting the impact of internal climate variability (Vaittinada Ayar et al., 2021; Jain et al., 2023). Utilizing Single Model Initial-Condition Large Ensembles (SMILEs) in a new framework could reveal how internal climate variations may modulate future flood risk across SSA. SMILEs were specifically designed to quantify the impact of internal climate variations in climate change scenarios (Milinski et al., 2020; Maher et al., 2021; Suarez-Gutierrez et al., 2021; Deser and Phillips, 2023; Jain et al., 2023).

Here, we aim at estimating the combined and relative contributions of large-scale internal climate modes of variability on the observed and future seasonal frequency of flood hazard in SSA. The study is organized as follows. In Section 2, we present the data and methods. In Section 3, we identify the large-scale drivers of seasonal flood frequency across SSA and quantify their relative importance. In Section 4, we evaluate the potential for different sequences and phasing of these large-scale climate variations to modulate seasonal flood risks in SSA from one 30-year period to another over the 21st century using multi-model large-ensembles and a statistical modelling approach. Lastly, Section 5 summarizes the main results and discusses their broader implications.

2. Data and methods

2.1. Data

2.1.1. Observed streamflow and flood occurrence

We computed flood occurrence across SSA from a 65-year daily streamflow dataset (Ekolu et al., 2022). This dataset was curated from two main sources: i) daily river discharge data from the "Système d'Informations Environnementales sur les Ressources en Eaux et leurs Modélisations" (SIEREM: https://www.hydrosciences.fr/sierem/; Boyer et al., 2006), which is hosted by the French Institute for Research and Development (IRD) and ii) the Global Runoff Data Centre databases (GRDC; https://portal.grdc.bafg.de/). Using the SIEREM and GRDC databases, Ekolu et al. (2022) selected 661 stations, covering 65 years from 1950 to 2014 with a maximum of 60 % missing data (Fig. 1). The missing data were then reconstructed using a random forest algorithm. For details on the data and reconstruction quality control, selection process, and potential influences of human activities readers are referred to Tramblay et al. (2020a) and Ekolu et al. (2022). Following the classification provided by FAO-GeoNetWork, Fig. 1 shows the spatial distribution of the major hydrological basins, as well as the number of stream gauges associated with their respective sub-catchments across SSA.

2.1.2. Observed sea surface temperatures and climate indices

To examine the observed relationships between regional flood frequency and the large-scale climate modes of variability, we utilise the Extended Reconstructed SST version 5 (ERSST.v5; Huang et al., 2017), which is an observation-based global monthly SST gridded dataset. This dataset was produced by the National Oceanic and Atmospheric Administration (NOAA) using the International Comprehensive Ocean-Atmosphere Dataset (ICOADS) Release 3.0. It has a $2^\circ \times 2^\circ$ resolution and covers the period from January 1854 to present, with enhanced representations of SST spatial and temporal variability compared to previous versions of this dataset (Huang et al., 2017). Unlike other observed SST datasets, ERSST.v5 is not impacted by cold SST biases brought on by the assimilation of satellite data at the end of the 20th century, which can occasionally result in a spurious mild slowdown in the global warming trend and problematic negative decadal signals (Reynolds et al., 2002).

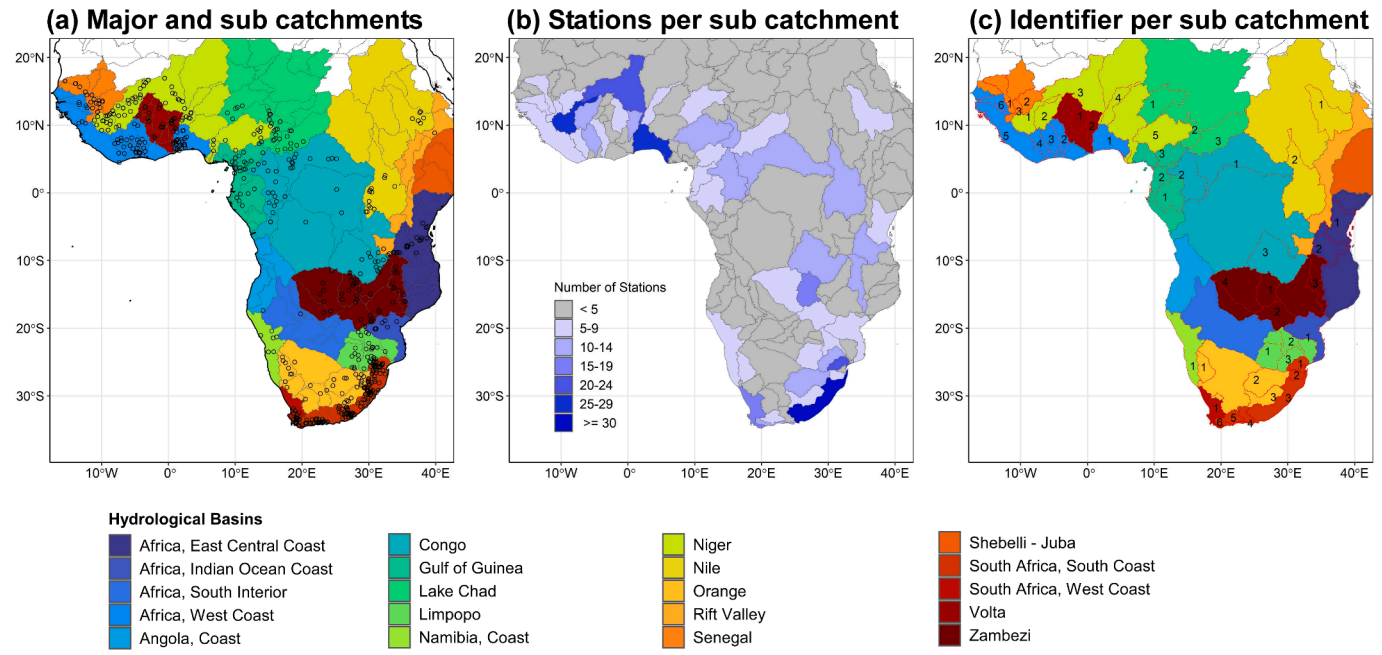

Fig. 1. Major hydrological basins and the number of stream gauges associated with their respective sub-catchments across SSA. a) Complete daily streamflow data from Ekolu et al. (2022) (black hollow circles), with corresponding major hydrological basins (colour shading) and sub-catchments (grey contours) in SSA. b) Total number of stations per sub-catchment in SSA. Shapefiles of major hydrological basins and sub-catchments are derived from FAO-GeoNetWork (https://www.fao.org/land–water/databases-and-software/geonetwork/en/; accessed in August 2022). c) Identifier for sub-catchments with 5 stations or more.

Using ERSST.v5, we calculated 16 climate indices (Table 1), which reflect well-known teleconnections between SSTa, rainfall and streamflow variability in SSA (*e.g.,* Fontaine et al., 2011; Rodríguez-Fonseca et al., 2015; Dieppois et al., 2013, 2015; 2016; Sidibe et al., 2019). Each climate index is calculated by taking the area weighted average SSTa over the corresponding SST regions (Table1). We use locally estimated scatterplot smoothing (LOESS) functions to suppress the seasonal cycle and detrend the SSTa data prior to calculating the indices. We then calculated the seasonal averages (*i.e.,* DJF, MAM, JJA and SON) of each climate index.

2.1.3. Climate models

To estimate potential future impacts of climate variability and change on regional and seasonal flood occurrence across SSA, we calculate the 16 climate indices in Table 1 using 12 Single Model Initial-condition Large Ensembles (SMILEs; from 6 to 100 ensemble members in each model) from the Coupled Model Intercomparison Project phases 5 and 6 (CMIP5 and 6), totalling 400 realizations of historical and future climate (1850–2005/14 and 2006/15–2100; Table 2). To examine the future period, we use the highest emission scenario or forcing level (8.5 $W.m^{-2}$), *i.e.,* Representative Concentration Pathway RCP8.5 in the CMIP5 models, and the Shared Socio-economical Pathway 5 that updates the highest forcing level, *i.e.,* SSP5-85, in the CMIP6 models. Using SMILEs permits more robust estimates of the combined effects of internal climate variations and externally forced changes that are directly associated with rising greenhouse gas concentration in the atmosphere (*e.g.,* Deser et al., 2012; Kay et al., 2015; Maher et al., 2019; Lehner et al., 2020).

To isolate the role of internal climate variations across the different ocean basins in each SMILE, we calculated monthly SSTa by subtracting the ensemble means of sea surface temperatures from all individual ensemble members, at each grid-point and on a monthly scale. By subtracting the ensemble means, which represent the externally forced signal and trends, to estimate SSTa associated with internal climate modes of variability. We also reduce the impact that other emission scenarios or forcing levels could have had on our results (*e.g.,* Deser et al., 2014, 2023). For instance, following the same approaches, Maher et al. (2023) and Cai et al. (2022) found very similar changes in the projected ENSO variations across different emission scenarios.

2.2. Methods

2.2.1. Identifying independent flood peak events

The most common way to analyse changes in the number of flood events is the Peak-over-Threshold (POT) approach. This method identifies floods as streamflow events above a specified threshold. However, the examination of floods assumes that flood occurrences are identically distributed and independent (WMO, 2009). Baseflow separation methods are the most used approach for identifying individual flow events and when combined with a flood selection criterion they allow for the identification of individual flood events. Different baseflow separation methods exist (*e.g.,* Nathan and McMahon, 1990; Tallaksen, 1995; Blume et al., 2007; Mei and Anagnostou, 2015), and here we adopt an automated baseflow separation using a digital filter method combined with a POT approach.

We first estimate the recession constant k for each station using the approach suggested in Vogel and Kroll (1996) and implemented in recent studies (*e.g.,* Thomas et al., 2013; Mangini et al., 2018; Ekolu et al., 2022). We achieve this by computing the 3-day centred moving average of the daily streamflow at each station from 1950 to 2014. Then, we locate the recession period, which begins from a given peak in this 3-day centred moving average time series and continues until the point where the flow suddenly increases. Subsequently, identification of recession events is repeated for each peak in the 3-day centred moving average time series. Note that only recession events longer than 10 days are selected.

We then calculate the recession constant for each recession event by applying regression analysis to find the best fit using ordinary least squares, as described in Equation (1). We compute the average recession constant across all recession events from 1950 to 2014. In this context, Q_t represents the total flow at any given time t, and Q_0 is the initial flow at the start of the recession period, with k_i being the recession constant.

$$In(Q_t) = In(Q_0) + In(k_i) \times t + r \quad (1)$$

Table 1
Detailed information for 16 SST indices.

Region	Indicator	Definition	References
Pacific Ocean	Nino34	Nino34 SSTa (−5°- 5°N, 190° − 240°E)	Rasmusson and Carpenter (1982)
	E	Eastern Pacific ENSO (Nino12 − [0.5 × Nino4]; Nino12 [0-10°S, 80°-90°W] Nino4 [-5-5° N, 160E-150 W])	Takahashi et al. (2011)
	C	Central Pacific ENSO (1.7 × Nino4 − [0.1 × Nino12])	Takahashi et al. (2011)
	TPI [IPV]	Tripole index of Pacific SSTa [Interdecadal Pacific Variability] (−50°- 45°N, 140° − 270°E)	Henley et al (2015)
	NP [PDV]	North Pacific SSTa [Pacific Decadal Variability] (20°- 65°N, 100° − 260°E)	Mantua et al. (1997)
Atlantic Ocean	TSA	Tropical South Atlantic SSTa (−20°- 0°N, −30° − 10°E)	Enfield et al. (1999)
	TNSD	Atlantic Meridional Mode (Difference between Tropical North [5°-25°N, −55° − −15°E] and South Atlantic SSTa [-20°- 0°N, −30° − 10°E])	Enfield et al. (1999)
	SAOD	South Atlantic Ocean Dipole (3rd PC tropical Atlantic SSTa: −30°- 30°N, −70° − 20°E)	Enfield et al. (1999)
	NA [AMV]	North Atlantic SSTa [Atlantic Multidecadal Variability] (0°- 60°N, −80° − 0°E)	Enfield et al. (2001)
Mediterranean Sea	EMED	East Mediterranean SSTa (32°- 44°N, 15° − 36°E)	Fontaine et al. (2011)
	WMED	West Mediterranean SSTa (32°- 44°N, −6° − 15°E)	Fontaine et al. (2011)
Indian Ocean	SWIO	South-West Tropical Indian Ocean SSTa (–32-25°N, 31° − 45°E)	Fontaine et al. (2011)
	TIO	Tropical Indian Ocean SSTa (−24°- 24°N, 35° − 90°E)	Fontaine et al. (2011)
	WTIO	West Tropical Indian Ocean SSTa (−10°- 10°N, 50° − 70°E)	Fontaine et al. (2011)
	DMI	Dipole Mode Index (Differences between West [-10°- 10°N, 50° − 70°E] and South-East Tropical [-10°- 0°N, 90° − 110°E] Indian Ocean SSTa)	Saji et al. (1999)
Globe	GT	Global SSTa (−70-70∘N)	Trenberth and Shea (2006)

Using the estimated recession constant k, we calculate the baseflow using the digital filter in Equation (2) by Chapman and Maxwell (1996). We then subtract the baseflow from the total flow to obtain the estimated direct flow. Independent discharge events are separated by intervals during which direct runoff is lower than the baseflow, or lower than the mean annual direct runoff. Where $Q_{b(i-1)}$ is the baseflow at time interval *i-1*, $Q_{d(i)}$ is the direct runoff at time interval *i*, and k is the recession constant.

$$Q_{b(i)} = \frac{k}{2-k} \times Q_{b(i-1)} + \frac{1-k}{2-k} \times Q_{(i)} \quad (2)$$

Following the identification of independent discharge peaks across the whole time series, flood series are compiled using the POT selection approach. This is done by ranking flow events from highest to lowest, and subsequently selecting the highest 195 events based on a POT criterion of three events per year over 65 years for each station. We provide an illustrative application of the baseflow separation and event identification methodology in the supplementary materials, focusing on a station located in the Congo basin (Fig. S1). To demonstrate the robustness of our chosen threshold, we evaluate the Spearman's correlation between the seasonal number of flood events identified using different POT thresholds (0.5, 1, and 2 events per year) compared to the chosen threshold of three events per year. These results, presented in Figure S2, revealed a high correlation ($\rho > 0.8$) across most stations, indicating consistent variability in flood occurrence regardless of the specific threshold within a reasonable range.

Table 2
Detailed information for the CMIP5 and CMIP6 climate models used in this study.

Model Version	Climate Model	Ensemble Members	References
CMIP5	CanESM2	49	Kirchmeier-Young et al. (2017)
–	CESM1-LE	40	Swart et al. (2019)
–	CSIRO-MK3	30	Jeffrey et al. (2013)
–	GFDL-CM3	20	Sun et al. (2018)
–	GFDL-ESM2M	30	Burger et al. (2022)
–	MPI-GE	100	Maher et al. (2019)
CMIP6	ACCESS-ESM1-5	10	Ziehn et al. (2020)
–	CanESM5	25	Swart et al. (2019)
–	GFDL-SPEAR-MED	30	Delworth et al. (2020)
–	IPSL-CM6A-LR	6	Boucher et al. (2020)
–	MIROC-ES2L	10	Hajima et al. (2020)
–	MIROC6	50	Tatebe et al. (2019)

In this study, we focus on the flood occurrence, which should be less sensitive to water management strategies and river regulation than flood magnitude and duration, hence providing more robust results. For instance, Brunner (2021) pointed out that flood management infrastructure (*e.g.,* reservoirs) reduce the severity of a flood by distributing the flow over a longer period. Each year, we calculate the seasonal total number of flood events (*i.e.,* from December-February [DJF] to September-November [SON]), which include a mixture of flood events, with lower and higher magnitude and duration at the sub-catchment scale, between 1950 and 2014. Nevertheless, we found significant and high correlations ($\rho > 0.8$) between the seasonal number of floods and the seasonal maximum magnitude and duration of floods at the sub-catchment scale (Fig. S3). This suggests that periods with higher (lower) number of floods are associated with higher (lower) maximum magnitude and duration of floods, and potentially similar large-scale climate drivers.

2.2.2. *Identifying large-scale climate drivers of long-term variations in seasonal flood hazards*

We examine the statistical relationships between large-scale climate variations and sub-catchment scale flood occurrence. We first analyse Spearman's rank correlations applied to four seasons (DJF, MAM, JJA and SON) and at multiple lag-times (climate indices with 0-, 3-, 6-, 9-month lag). We then select the most relevant set of climate indices and lag-times. Next, we reduce the number of variables by fitting a stepwise generalized linear model (GLMs) with a Poisson distribution. Finally, we quantify the combined and relative contributions of large-scale drivers to the seasonal and regional flood occurrences. This is first achieved using a stepwise model selection based on Akaike information criterion (AIC) to reduce the set of potential large-scale climate predictors after considering multicollinearity (Sauerbrei and Schumacher, 1992; Smith, 2018). Secondly, we evaluate the relative contribution of the selected set of large-scale predictors using a dominance analysis, consisting of decomposing the coefficients of determination (R2) and quantifying the contribution of each regressor to the total R2 of the fitted GLM (Budescu, 1993; Azen & Budescu, 2003; Azen and Traxel, 2009; Luo and Azen, 2013). Note that to assess the sampling uncertainty, we use 1000 bootstraps in the stepwise model selection and

in the dominance analysis. In addition, we test the statistical significance of the GLM results for each sub-catchment and season using a Chi-square test at $p \leq 0.05$.

2.2.3. *Estimating future impacts of large-scale climate variations on regional flood hazards*

To estimate how large-scale climate variations could potentially alter the future occurrence of flooding during the 21st century (2015–2100), we use the same GLM models previously developed (see Section 2.2.2), but with climate indices derived from 12 CMIP5 and CMIP6 SMILEs as large-scale predictors (totalling 400 realisations of past, present, and future climate). This statistical framework enables us to estimate how different sequences of internal climate variability, reflecting the divergent phases of the large-scale climate predictors (*e.g.,* ENSO, AMV) in different climate models, or in different realisations of the same model, can affect the seasonal number of floods in 48 SSA sub-catchments between 1950 and 2100.

For each model simulation, sub-catchment, and season, we compute the rolling 30-year average of the simulated number of floods generated as a result of future variations in the large-scale climate modes. Next, we standardise the relative change in the future number of floods across the different SMILEs, to facilitate cross-comparisons. For each season, we do this by first subtracting the simulated historical mean number of floods (1985–2014) from each future 30-year rolling mean number of floods. Then, we divide this difference by the simulated historical mean number of floods and express the resulting ratio as a percentage.

The potential range of impacts of large-scale climate modes of variability on the future number of floods is assessed by identifying the maximum and minimum plausible changes across all SMILEs. For each sub-catchment and season, the 90th percentile (representing the maximum plausible increase) and the 10th percentile (representing the maximum plausible decrease) of the standardized seasonal mean number of future floods are calculated across all SMILEs. Finally, we evaluate the potential range of future variability in the seasonal mean number of floods by computing the standard deviation of the standardized seasonal mean number of floods across all SMILEs.

In the present study, we first consider all CMIP5 and CMIP6 models as equal in their representations of large-scale climate modes of variability. However, recent studies show contrasting performance in representations of ENSO, PDV and AMV (Dieppois et al., 2021; Fasullo et al., 2020; Coburn and Pryor, 2021). Therefore, we also compare the relative standard deviation of the standardized mean number of floods simulated in individual CMIP5 and CMIP6 SMILEs to assess whether some models produce unrealistically high and/or low range of variations in flood hazards in response to the same large-scale climate modes of variability.

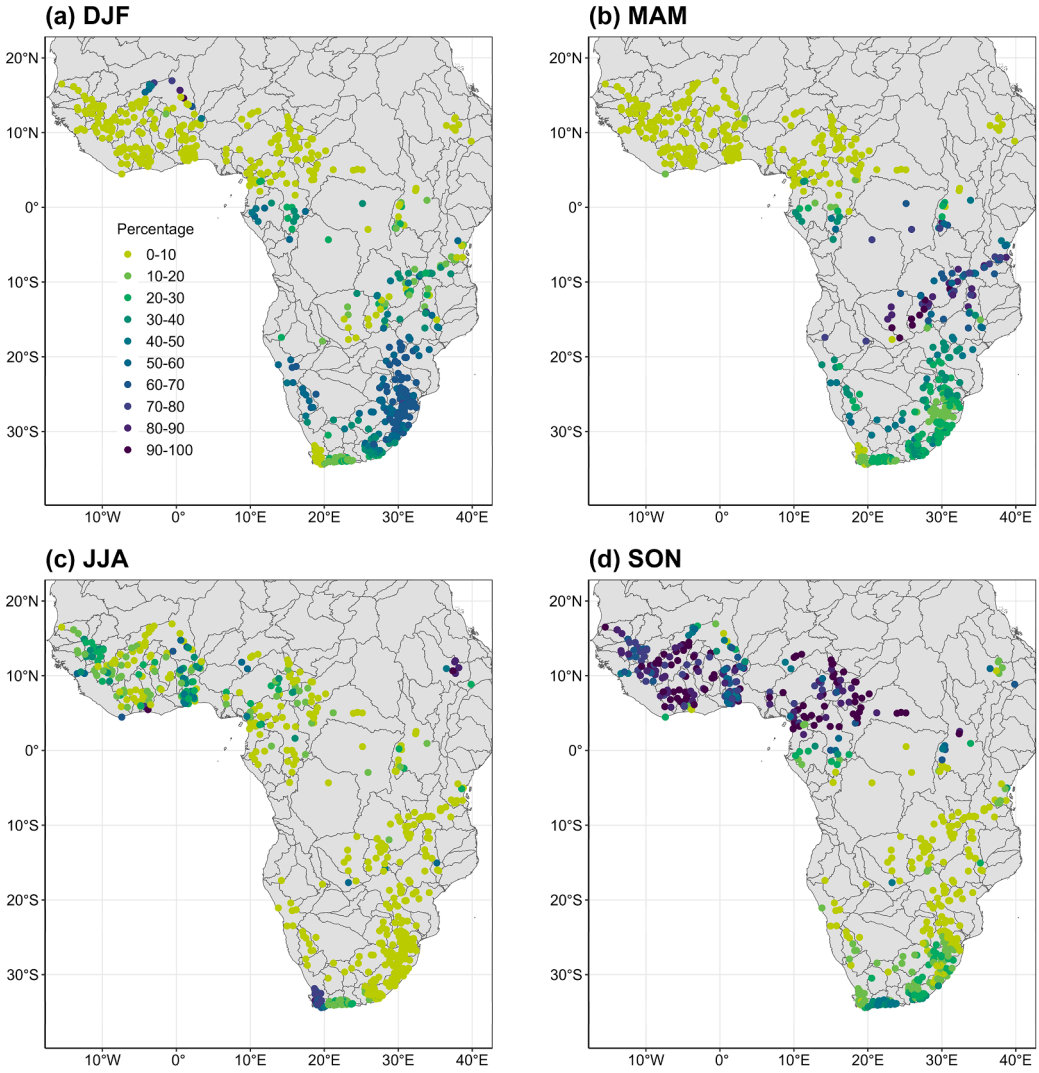

Fig. 2. Relative percentage of seasonal flood occurrences between 1950 and 2014 in SSA. a) Mean percentage of floods occurring in DJF compared to the annual average number of floods between 1950 and 2014. b-d) Same as a) but for MAM, JJA and SON.

3. Results

3.1. Seasonal changes in flood hazard

Flood occurrence in SSA shows considerable seasonal variability (Fig. 2). The northwest regions of southern Africa experience more flood events when the Inter-Tropical Convergence Zone (ITCZ) is at its southernmost position in DJF, compared to other seasons (Fig. 2a). This region of southern Africa, which is also known as the summer-rain region (Tyson et al., 2000; Roffe et al., 2019), receives up to 60–70 % of floods in DJF, and between 10–30 % of floods in MAM (Fig. 2b). Meanwhile, the winter-rain region of southern Africa (*i.e.,* the south-western cape) shows a seasonal peak in flood occurrence in JJA (Fig. 2c).

In MAM, as the ITCZ starts its northward progression, the south-eastern equatorial regions of East Africa (Zambezi; Fig. 2b) experience more flooding compared to other seasons. The south equatorial regions of East Africa (Zambezi), which typically receive most of their rains between October and March (Liebmann et al., 2012; Dunning et al., 2016; Nicholson and Selato, 2000), have between 50 and 80 % of the floods occurring in MAM and between 30 and 40 % in SON (Fig. 2b).

The northern regions of East Africa (*e.g.,* Blue Nile [Nile-1]) register between 80 and 90 % of flood occurrences in JJA, when the ITCZ is approaching its northernmost position (Conway, 2005; Leggesse and Beyene, 2017). West Africa also records a substantial fraction of floods in this season (30–40 %; Fig. 2c). However, most flood events in West Africa (70–80 %) occur in SON (Fig. 2d), following the core of the Sahelian rainy season in August (Thorncroft et al., 2011; Vizy & Cook, 2018). Interestingly, the middle Niger catchment in West Africa shows seasonal peaks in flood occurrence in DJF (Fig. 2a). Some Sahelian catchments have two flood peaks (Descroix et al., 2013; Casse et al., 2016): i) the Sahelian flood, which occurs during the Sahelian monsoon season (July to September) due to inflows from the right bank tributaries upstream of Niamey; and ii) the Guinean flood, which occurs when the rain belt retreats south (November and February), due the delayed arrival of floods from the upper part of the Niger.

In summary, as noted in Ficchì and Stephens (2019), the occurrence and timing of floods in SSA have a close spatial and temporal relationship with that of rainfall and follow the ITCZ seasonal patterns.

3.2. Observed statistical relationships between seasonal flood hazard and large-scale climate drivers

We have shown that, compared to other seasons, the summer-rain region of southern Africa experiences the highest frequency of flood events in DJF and MAM (Fig. 2a-b). In this region, floods show significant negative correlations with SSTa in the equatorial Pacific Ocean (notably, Nino34, C and TPI) and the Indian Ocean (TIO, WTIO and DMI; Fig. 3a-b). During the same seasons and in the same region, there are significant positive correlations between flood occurrences and the North and Tropical Atlantic Ocean (AMV and TNSD) and eastern Mediterranean Sea (EMED; Fig. 3a-b). This suggests that warmer (cooler) Pacific and Indian Ocean, and reversely cooler (warmer) North Atlantic Ocean and eastern Mediterranean, disfavour (favour) the occurrence of floods in the summer-rain region of southern Africa. This is consistent with previous studies on southern African rainfall, highlighting the role of ENSO and its interactions with the Indian Ocean, the North and Tropical South Atlantic (*e.g.,* Washington and Preston, 2006; Lyon and Mason, 2007; Hoell et al., 2015; Dieppois et al., 2016, 2019; Hoell and Cheng, 2018; Pohl et al., 2018; Ullah et al., 2022). Consistent with previous studies on the link between ENSO and rainfall in the winter-rain region of southern Africa (*e.g.,* Dieppois et al., 2016), we find that ENSO is also linked to flood occurrence in JJA in this region (*i.e.,* South Africa, West Coast; Fig. 3c). In southern Africa, winter rainfall variability is indeed strongly related to regional changes in midlatitude frontal activity, which is typically associated with dipolar SSTa in the Indian and South Atlantic Oceans (Reason and Rouault, 2005; Dieppois et al., 2016). Nevertheless, according to Philippon et al. (2012), the significant influence of ENSO may only emerge after the 1970 s over this region.

Concerning East Africa, in the White Nile (Nile-2) and the Africa East Central Coast catchments, floods are significantly positively correlated with SSTa in the equatorial Pacific (Nino34, C, and TPI), the Indian Ocean (SWIO, TIO and WTIO), the South Atlantic Ocean Dipole (SAOD) in MAM (Fig. 3b). This suggests that warmer (cooler) SSTa over these ocean basins are likely to lead to more (fewer) floods in the region. This is consistent with previous studies discussing the role of climate variations in the Atlantic Ocean (*e.g.,* Camberlin and Okoola, 2003; Williams et al., 2012), ENSO (*e.g.,* Janowiak, 1988; Ogallo, 1988; Mutai et al., 1998; Reason et al., 2000; Giannini et al., 2008; Parhi et al., 2016), and the Indian Ocean Dipole (*e.g.,* Saji et al., 1999; Webster et al., 1999; Black et al., 2003; Manatsa et al., 2012; Manatsa and Behera, 2013) on eastern African rainfall. Meanwhile, in the boreal summer (JJA), when the Blue Nile receives more floods compared to the rest of the year (Fig. 2c), our results show negative correlations between the number of floods and climate variations in the equatorial Pacific Ocean (Nino34, E, C and TPI), and the Indian Ocean (WTIO and DMI; Fig. 3c). At the same time, we find positive correlations with SSTa in the Atlantic Ocean (TNSD and AMV) and the eastern Mediterranean Sea (EMED). This is consistent with previous studies on rainfall-SSTa teleconnections in this region of eastern Africa, which highlight significant differences in the tropical dynamics and environmental factors (topography, lakes) affecting rainfall variability in the While and Blue Nile (*e.g.,* Camberlin, 1995, 1997; Segele et al., 2009; Nicholson and Selato, 2000; Williams et al., 2012; Omondi et al., 2013; Nicholson and Selato, 2000). El Niño (La Niña) episodes were shown to be associated with less (more) rainfall in the Blue (White) Nile (*e.g.,* Camberlin, 1995, 1997; Nicholson and Selato, 2000; Segele et al., 2009; Nicholson et al. 2017). Meanwhile, Williams et al. (2012) and Omondi et al. (2013) found contrasted teleconnections between seasonal rainfall and the Indian and Atlantic Oceans over the White and Blue Nile regions.

Regarding western and central Africa in JJA and SON, we find that floods are positively correlated with SSTa in the Mediterranean Sea (WMED and EMED), the Atlantic Ocean (AMV, TNSD and TSA), and the North Pacific Ocean (NP; Fig. 3c-d). Negative correlations are found with the Atlantic Ocean (SAOD and TSA), equatorial Pacific Ocean (Nino34, C and TPI) and Indian Ocean (SWIO, WTIO and TIO' Fig. 3c-d). This implies that a warmer (cooler) North Atlantic Ocean and Mediterranean Sea favour (disfavour) flood occurrences across most parts of western and central Africa. Meanwhile, a warmer (cooler) equatorial Pacific, South Atlantic and Indian Ocean disfavour (favour) flood occurrences. These statistical relationships thus appear consistent with existing literature on rainfall-SSTa teleconnections. For instance, cooler Tropical South Atlantic and warmer North Atlantic were found to favour rainfall in the West Africa Sahel (*e.g.,* Losada et al., 2010; Dieppois et al., 2013, 2014). Meanwhile, a warmer (cooler) Mediterranean Sea was found to be associated with increased (decreased) rainfall in the same region (*e.g.,* Rowell, 2013; Fontaine et al., 2010; Gaetani et al., 2010). Similarly, warmer temperatures in the equatorial Pacific and Indian Oceans were found to favour drought conditions in West Africa (*e.g.,* Giannini et al., 2005; Rodríguez-Fonseca et al., 2015; Sidibe et al., 2019), therefore disfavouring flood occurrences.

3.3. Combined and relative importance of large-scale climate drivers of long-term variations in seasonal flood hazards

In Fig. 4, we quantify the overall and relative contributions of large-scale climate modes to year-to-year variations in flood occurrence across SSA, using stepwise GLM regression models and dominance analysis. We find that the combined impact of large-scale climate modes of variability explains 30–90 % of the fluctuations observed in floods across SSA. We also note that the contribution of large-scale climate modes to seasonal flood occurrences are higher in western, central and southern Africa

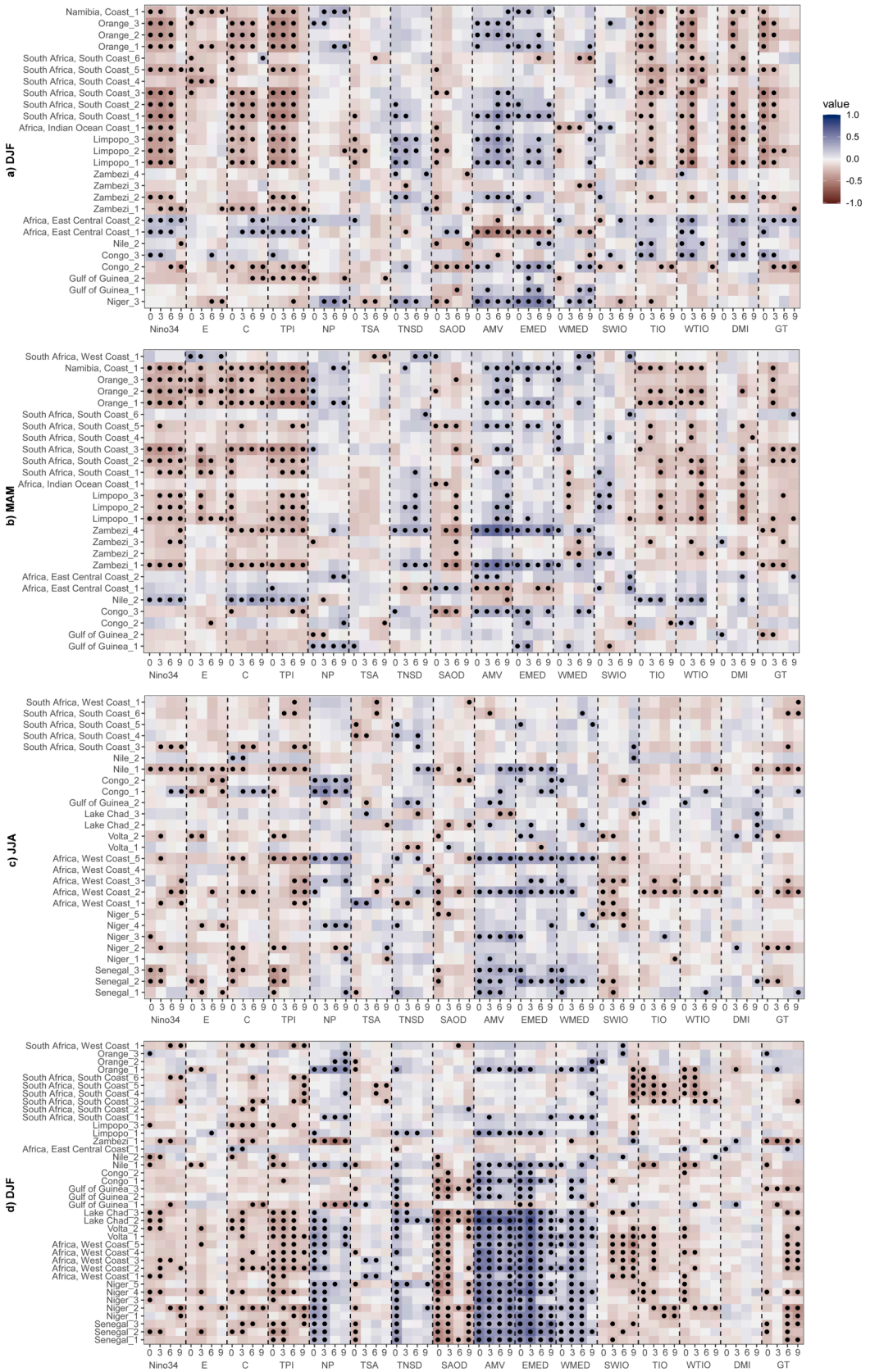

Fig. 3. Statistical relationships between large-scale climate indices and seasonal flood occurrences in SSA. a) Spearman's correlation between large-scale climate indices (x-axis; [left to right]: Nino34, E, C, TPI, NP, TSA, TNSD, SAOD, AMV, EMED, WMED, SWIO, TIO, WTIO, DMI, GT) and the number of floods occurring in DJF at the sub-catchment scale (y-axis) using four different lag-times (0-, 3-, 6,- 9-month). b-d) Same as a) but for MAM, JJA, and SON. Black dots indicate Spearman's correlations that are significant at $p \leq 0.05$. Note that on each panel, only sub-catchment experiencing at least 10 % of their annual total amount of floods during the corresponding seasons are shown.

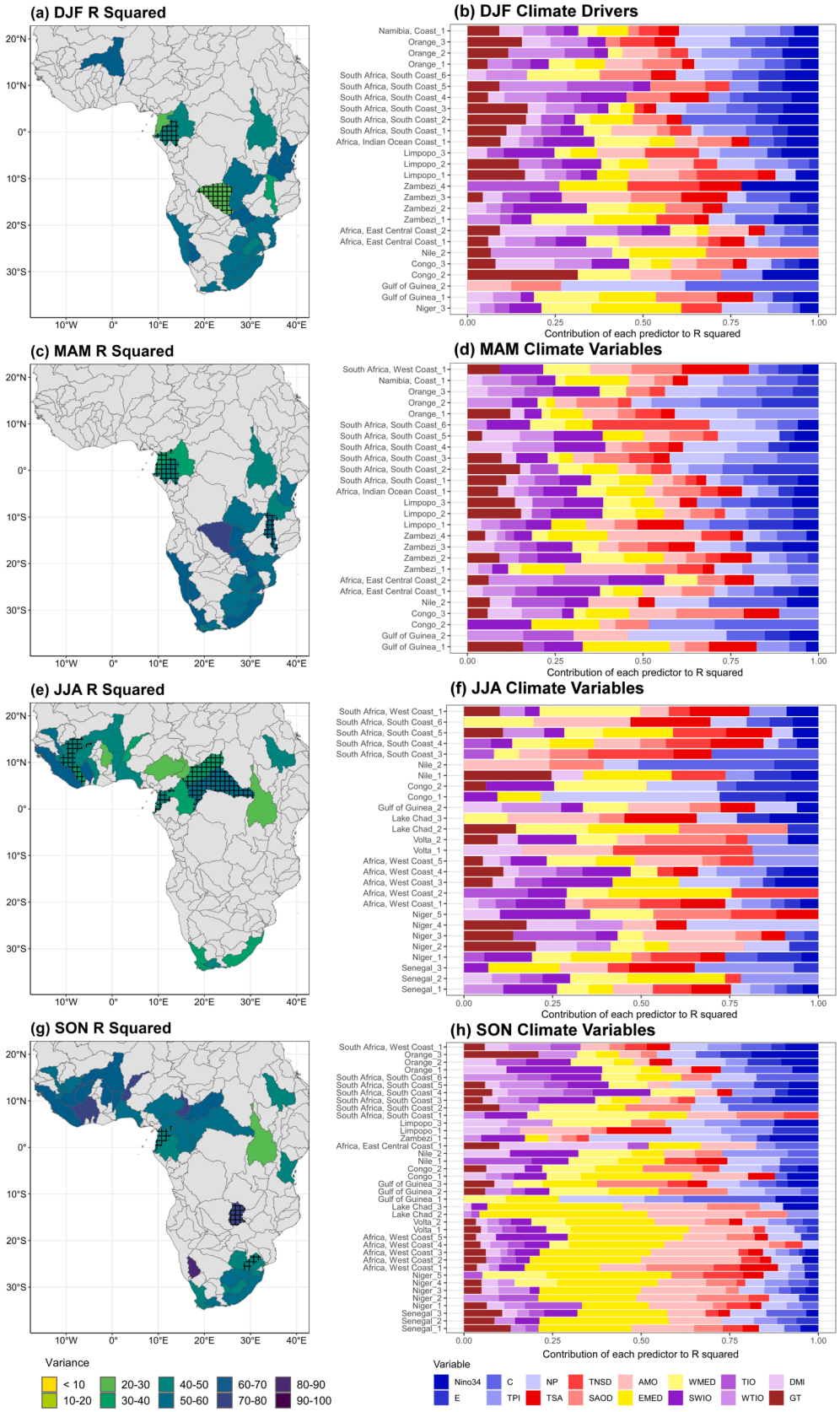

(caption on next page)

Fig. 4. Combined and relative importance of the large-scale drivers in modulating seasonal flood occurrences in SSA between 1950 and 2014. a) Combined and b) relative importance of large-scale climate indices to year-to-year variations in the number of floods in DJF, here quantified though the total R2 expressed as a percentage from the corresponding GLM models, and by decomposing/quantifying the contribution of each regressor (climate indices) to the total R2 using dominance analysis, respectively. Panels c-d), e-f), and g-h) are the same as panels a-b) but for MAM, JJA, and SON, respectively. On the left panels, hatching indicates sub-catchments where the total R2 expressed by the GLM models is not significant according to a chi-square test at $p \leq 0.05$. On the right panels, only sub-catchments receiving at least 10 % of their total number of floods during the corresponding seasons are displayed.

than in eastern Africa.

In DJF, when most floods occur in the summer-rain region of southern Africa (Fig. 2a), the overall contribution of the large-scale climate modes to southern African flood variability lies between 50 and 60 % (Fig. 4a). We also note that the largest contribution to flood variability is found in the Pacific Ocean (~14–25 %: Nino34, TPI and NP), followed by the Indian Ocean (~7.0–20 %: SWI, DMI and TIO) and the Atlantic Ocean (~5–10 %: AMO, TNSD and SAOD; Fig. 4b). While in line with previous research highlighting the importance of the combined impacts of the Pacific, Atlantic and Indian Oceans in modulating rainfall amount (*e.g.,* Washington and Preston, 2006; Lyon and Mason, 2007; Hoell et al., 2015; Dieppois et al., 2016, 2019; Hoell and Cheng, 2018; Pohl et al., 2018; Ullah et al., 2022) and thus flood hazards, these findings also emphasize the primary importance of the Pacific Ocean in triggering changes in water supply and flood risks in the summer-rain region of South Africa. Interestingly, in MAM, we also find that the same set of large-scale climate modes shows a larger contribution (*i.e.,* 70–80 %) to variations in flood occurrences over the same region (Fig. 4c-d). This is consistent with, Monerie et al. (2019), who suggested that the impact of, and the predictability conferred by, ENSO was larger over Mozambique than in South Africa.

On the contrary, and consistently with previous studies (*e.g.,* Reason and Rouault, 2005; Dieppois et al., 2016), the importance of large-scale variations in the SSTa in modulating the occurrence of floods is lower over the winter-rain region of southern Africa. Our analysis reveals that large-scale climate modes explain 30–40 % of the variations in flood occurrence in the winter-rain region of southern Africa (Fig. 4e). In addition, the relatively low contributions of large-scale climate modes to variations in flood occurrence in the southwestern regions of South Africa (winter-rain regions) could reflect a much stronger influence of human activities (*e.g.,* dams, irrigation, groundwater extraction; Chawanda et al., 2020). Nevertheless, we note that the most important contributors to flood variations are linked to changing SSTa in the North and Tropical South Atlantic Ocean (11 %: AMV and TSA), the western Mediterranean Sea (10 %: WMED), which may share some variations with the North Atlantic Ocean, and Pacific Ocean (7.0 %: Nino34 and TPI; Fig. 4f). Meanwhile, the Indian Ocean explains a smaller amount of variance of flood occurrences (4 %: SWIO and DMI).

In East Africa (*i.e.,* Zambezi, White Nile, and the Africa East Central Coast), large-scale climate modes only explain between 30 and 50 % of the variability in the number of floods during MAM. In this region, changes in the Pacific Ocean (~17–20 %: Nino34 and TPI) seem to be the primary driver of flood variations, compared to the Indian Ocean (~7–15 %: SWI, DMI and TIO) and Atlantic Ocean (~5–15 %: AMV, SAOD and TSA). Regarding the Blue Nile, where most yearly flooding occurs in JJA, the amount of flood variability linked to changes in large-scale climate variability is 48 % (Fig. 4e). Most of this variability is statistically linked to changes in the global ocean temperature (13 %: GT), the Pacific Ocean (12 %: C, Nino34 and NP), Atlantic Ocean (7.5 %: TNSD), Mediterranean (12 %: EMED) and Indian Ocean (4.5 %: DMI; Fig. 4f). This is thus consistent with Omondi et al. (2013) and Segele et al. (2009), who showed that the main rainfall season of Ethiopia is influenced by all three oceans (Pacific, Atlantic and Indian Oceans) and particularly by ENSO.

In western and central Africa, the total variance of flood occurrence that is linked to changes in large-scale climate variability is very high in SON (~70–90 %; Fig. 4g). During this season, the Atlantic Ocean (~9–30 %: AMO and TSA) and the Mediterranean Sea (~13–32 %: EMED) are the main large-scale drivers of year-to-year variability in flood occurrence in West and Central Africa (Fig. 4h). The Pacific Ocean (~3–17 %: Nino34, NP and TPI) and Indian Ocean (~3–19 %: SWIO, WTIO and DMI) contribute a minor amount to the overall variability (Fig. 4h). Our findings are in line with Chun et al. (2021), who found that variations in annual maximum flow in the Niger and Senegal River are primarily affected by the SSTa in the eastern Mediterranean Sea and the Atlantic Ocean, while the Pacific and Indian Ocean plays a secondary role.

3.4. *Estimating future impacts of large-scale climate variations in regional flood hazards*

Here, we use the statistical model developed in the previous section to estimate how, in CMIP5 and CMIP6 SMILEs, different sequences of internal variability, affecting the phasing and amplitude of key climate modes (*e.g.,* ENSO, AMV), can alter the number of floods from one 30-year period to another during the 21st century in 48 sub-catchments in SSA. In Fig. 5, we illustrate how for an example sub-catchment (upper Niger sub-catchment), the number of floods simulated in SON can vary from one 30-year period to another in relation to different phase and amplitude of key climatic modes during the 21st century in two different climate models (CanESM5 and GFDL-SPEAR-MED) and in two realisations of the same model (CanESM5 ensemble members 11 and 16). Comparing CanESM5 and GFDL-SPEAR-MED, we note that CanESM5 (GFDL-SPEAR-MED) shows two flood-rich and two flood-poor periods from the 1970 s to 1990 s and from the 2020 s to 2050 s (from 1990 s to 2020 s and from 2050 s to 2070 s), which correspond to different phasing of EMED, AMV, TIO and NP (Fig. 5b-c). During the flood-rich period, EMED, AMV and NP tend to be warmer, while TIO tend to be cooler and vice-versa during flood-poor periods. Similarly, comparing two realisations (or ensemble members) of the same climate model, we note that differences in the simulated number of floods, associated with different phasing and amplitude of internal modes of climate variability (Fig. 5e-f), can be remarkably like when comparing two different climate models (Fig. 5a, d).

Applying the same analysis to all SSA sub-catchments and using 12 CMIP5 and CMIP6 SMILEs, we analyse the 90th, 10th percentiles and the standard deviation, *i.e.,* the upper, lower bound and long-term variability in the probable impacts of future large-scale climate modes of variability on flood occurrence over a moving window of 30-years between 2015 and 2100 (Fig. 6). Overall, we find that different overlapping phases and amplitudes of key modes of large-scale climate variability could be associated with variation in the number of floods of approximately between ± 10 to ± 50 % on average from one 30-year period to another across SSA. However, the potential future impact of large-scale climate variability on flood frequency varies from one season to another.

In DJF, over the summer-rain region of southern Africa, different sequences of large-scale modes of variability in different CMIP5 and CMIP6 SMILEs could lead to potential increases (decreases) in the number of floods that range from + 21 and + 52 % (−17 and −37.5 %) from one 30-year period to another during the 21st century, as determined by the 90th (10th) percentile (Fig. 6a-b). In the same region, using different SMILEs, the future impacts of large-scale climate modes of variability are found to be associated with relative standard deviations in future flood occurrence that are ranging from + 16 to + 40 % across the sub-catchments from one 30-year period to another during

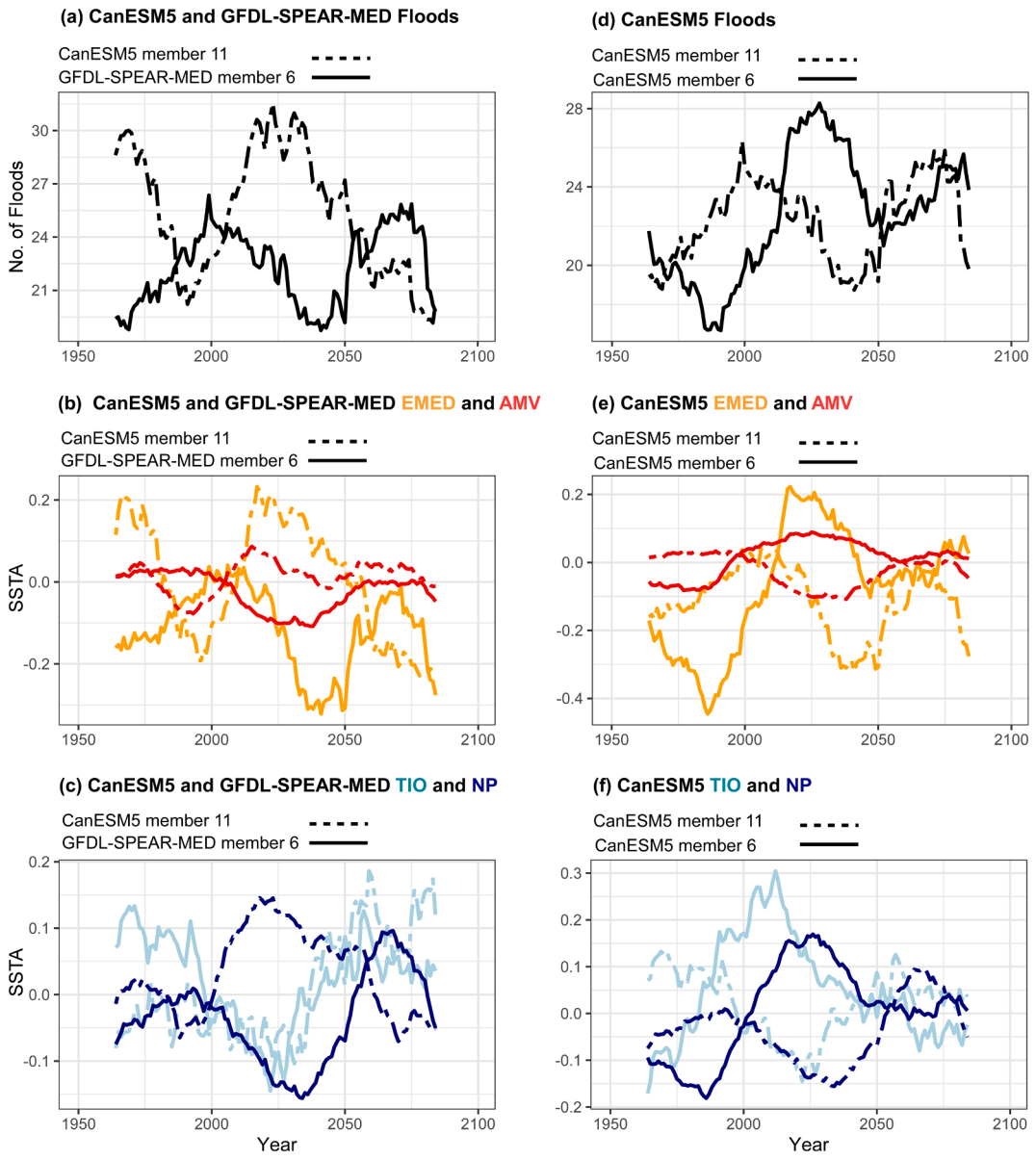

Fig. 5. Long-term changes in the number of floods in the Upper Niger sub-catchment (Niger_3) and associated changes in large-scale climate drivers in the Atlantic Ocean, Mediterranean Sea, Indian and Pacific Oceans. a) Thirty-year running mean of the simulated number of floods during SON in response to large-scale climate variations in the Upper Niger sub-catchment under two CMIP6 models: CanESM5 member 11 (model 1) and GFDL-SPEAR-MED member 6 (model 2). b) Thirty-year running mean of EMED and AMV indices in the same two CMIP6 models (CanESM5 member 11 and GFDL-SPEAR-MED member 6). c) Same as b) but for the TIO and NP climate indices. d-f) Same as a-c), but for two different ensemble members from CanESM5 (member 11 and member 16).

the 21st century (Fig. 6c). In the same region in MAM, future large-scale climate variations contribute to slightly greater ranges of variation in flood occurrences, especially in sub-catchments that tend to experience fewer floods during this time of the year (Fig. 6d-f). In the winter rain region of southern Africa, where more than 50 % of floods occur in JJA, the future impact of large-scale climate modes of variability in different CMIP5 and CMIP6 SMILEs is found to be associated with a relative standard deviation in future flood occurrence ranging from + 11 to + 25 % across sub-catchments from one 30-year period to another during the 21st century (Fig. 6g-i).

In MAM, in East Africa, especially over the White Nile and the Africa East Central Coast catchments, different phases and amplitudes of large-scale modes of variability in different CMIP5 and CMIP6 SMILEs could lead to potential increases (decreases) in the number of floods ranging from + 22.5 and + 33 % (−20 and −28 %) across catchments from one 30-year period to another during the 21st century, as determined by the 90th (10th) percentile (Fig. 6d-e). We also note that the future impacts of large-scale climate modes of variability are found to be associated with relative standard deviations in future flood occurrence ranging from 17 to 27 % across catchments from one 30-year period to another during the 21st century (Fig. 6f). Across the Blue Nile, in JJA, the future impacts of large-scale climate modes of variability are found to be associated with a relative standard deviation in future flood occurrence of 11 % from one 30-year period to another during the 21st century (Fig. 6g-i).

Over western and central Africa, in JJA and especially SON, different sequences of large-scale modes of variability in different CMIP5 and CMIP6 SMILEs could lead to potential increases (decreases) in the number of floods ranging from + 15 and + 88 % (−11 and −45 %) across catchments from one 30-year period to another during the 21st century, as determined by the 90th (10th) percentile (Fig. 6g-h, j-k). We also found that the future impacts of large-scale climate modes of variability

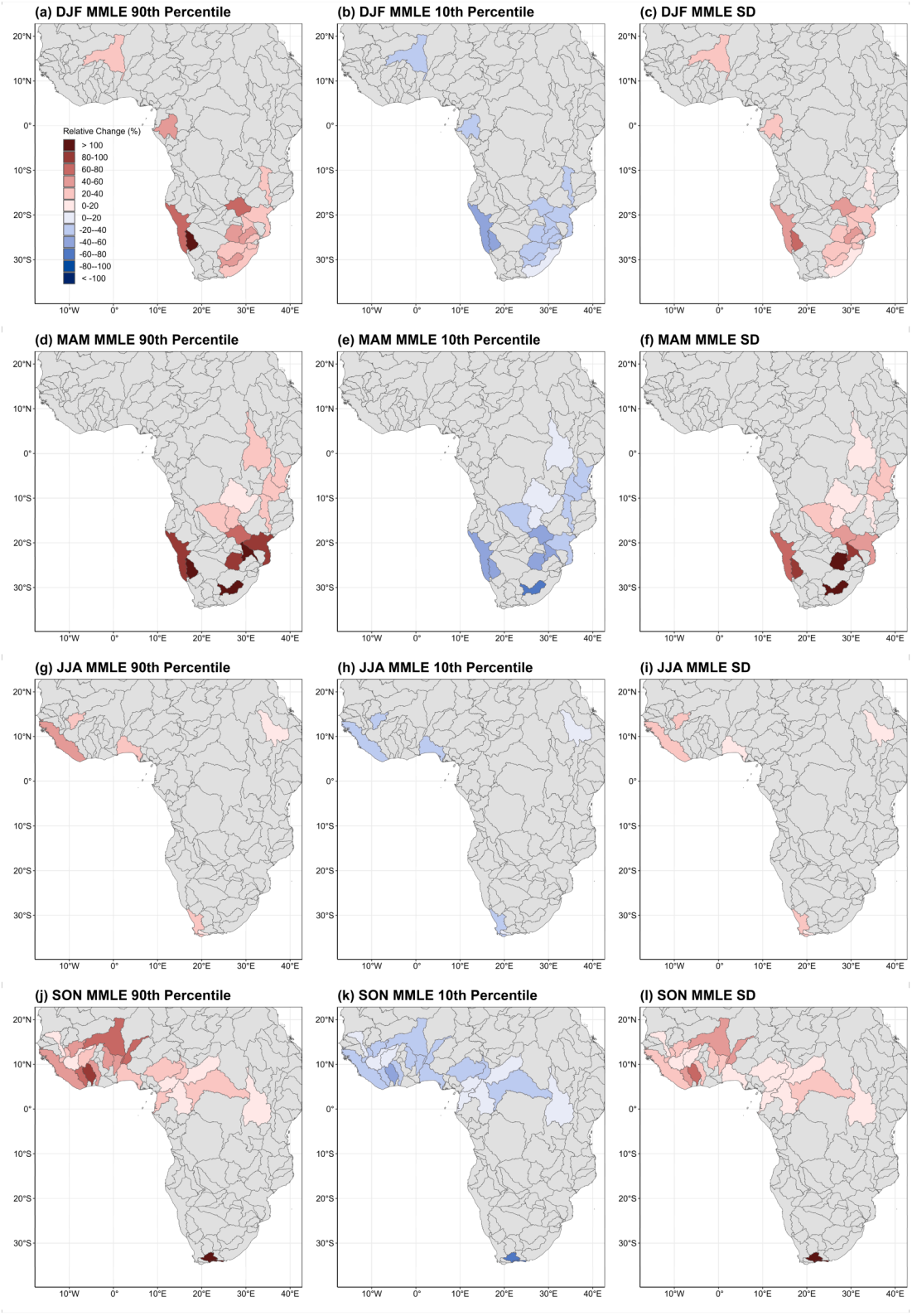

Fig. 6. Potential impact of sequences of large-scale climate variability on seasonal flood hazards in SSA during the 21st century. a-c) 90th and 10th percentiles (left and middle panels), as well as relative standard deviation (SD; right panel) of the projected impacts of large-scale climate variability on flood frequency across SSA in DJF in CMIP5 and CMIP6 SMILEs over all projected 30-year periods during the 21st century. d-f), g-i), and j-l) same as a-c) but for MAM, JJA and SON, respectively. The impact of large-scale climate variations on the number of floods is estimated using a stepwise generalized linear model based on a Poisson distribution. We then calculate the difference between simulated flood frequency over the historical period (1985–2014) and each future 30-year period (SSP-RCP5.85 scenarios: 2015–2100) in the 12 CMIP5-6 SMILEs (totalling 400 realisations). Note that on each panel, only the sub-catchments experiencing at least 30% of their annual total number of floods during the corresponding seasons are shown.

tend to be associated with a relative standard deviation in future flood occurrence ranging from 10 to 61 % from one 30-year period to another during the 21st century (Fig. 6i, l).

3.5. Differences between climate models in estimating future flood risk due to large-scale climate drivers

For each CMIP5 and CMIP6 SMILE, Fig. 7 shows the ensemble spread in the simulated impact of different sequences of climate variability on the number of floods between one 30-year period to another in the 21st century across SSA. We find that all CMIP5 and CMIP6 SMILEs show regionally consistent standard deviations in the impact of large-scale climate variability on the number of floods (Fig. 7a, c-d). For each season and region, the relative standard deviations in the simulated impact of large-scale climate variability on regional flood frequency only differ by 10 % on average from one climate model to another.

However, focusing on specific regions, we note non-negligible inter-model differences in the simulated impact of large-scale climate variations on flood hazard. For instance, in DJF and MAM over southern Africa, some models (*e.g.,* CSIRO-MK3, GFDL-CM3, GFDL-ESM2M, MIROC-ES2L) exhibits greater variability in flood hazard in response to large-scale climate variability compared to the other climate models (Fig. 7a-b). On the contrary, over the same season and regions, some models (*e.g.,* ACCESS-ESM1-5, CanESM5, IPSL-CM6A-LR) show lower variability in flood hazard in response to large-scale climate variability (Fig. 7a-b). These differences in the impact simulated by different groups of climate models are consistent with contrasted performance in simulating the variance of key climate modes of variability for southern African floods. For instance, some models underestimate (*e.g.,* GFDL-CM3 and GFDL-ESM2M) or overestimate (*e.g.,* CanESM5, and IPSL-CM6A-LR) the amplitude of ENSO variations (McKenna et al., 2020). Similarly, some models underestimate (*e.g.,* CSIRO-MK3, GFDL-CM3) or overestimate (*e.g.,* GFDL-ESM2M) the IPV and PDV on decadal timescales (Coburn & Pryor, 2021). In the Indian Ocean, some models overestimate (*e.g.,* CSIRO-MK3, GFDL-ESM2M, ACCESS-ESM1-5, CanESM5 and IPSL-CM6A-LR) or underestimate (*e.g.,* GFDL-CM3) the amplitude of IOD variations (McKenna et al., 2020).

Similarly, in JJA and SON, over western Africa, some models (*e.g.,* CSIRO-MK3, GFDL-CM3, GFDL-ESM2M, MIROC6, MPI-GE) show much higher variability in flood hazard in response to large-scale climate variability compared to the other climate models (Fig. 7c-d). Conversely, other models (*e.g.,* MIROC-ES2L, ACCESS-ESM1-5, CanESM5, IPSL-CM6A-LR) show much lower variability in flood hazard in response to large-scale climate variability (Fig. 7c-d). These differences in the impact simulated by different groups of climate models are consistent with contrasted performance in simulating the variance of the AMV (Coburn & Pryor, 2021; Richter & Tokinaga, 2020), which appear to be underestimated in some models (*e.g.,* CSIRO-MK3, GFDL-CM3, MPI-GE, ACCESS-ESM1-5, IPSL-CM6A-L and MIROC-ES2L) or overestimated in others (*e.g.,* GFDL-ESM2M, CanESM5).

4. Discussion and conclusions

This study aims to estimate and understand the combined and relative contributions of large-scale climate modes of variability in modulating the frequency of seasonal flood occurrence in the observed and future climates in SSA. While some previous studies have attempted to characterize past changes in floods in SSA (*e.g.,* Descroix et al., 2013; Nka et al., 2015; Aich et al., 2016; Do et al., 2017; Wilcox et al., 2018; Degefu et al., 2019), these endeavours have been generally limited to the catchment scale, obscuring broader climatic influences on several catchments in a given region (Kingston et al., 2020).

Using a 65-year daily streamflow dataset, covering over 600 catchments of SSA (Ekolu et al., 2022), we examine the relationship between large-scale climate variability and regional/seasonal flood occurrence. Despite potential impacts of human activities (*e.g.,* dams, irrigation, groundwater extraction) on the detection of flood events (Chawanda et al., 2020), we find significant statistical relationships between flood occurrences and large-scale modes of climate variability across all regions of SSA, consistent with previous studies on rainfall (*e.g.,* Fontaine et al., 2010; Rodríguez-Fonseca et al., 2015; Hoell et al., 2015; Dieppois et al., 2016; Parhi et al., 2016; Nicholson, 2017; Sidibe et al., 2019). To further understand the combined and relative importance of each mode of large-scale climate variability in modulating seasonal and regional flood occurrence, we use stepwise regressions and dominance analysis. This analysis revealed that the combined impact of large-scale climatic drivers can explain between 30 and 90 % of the observed variability in flood occurrences across SSA between 1950 and 2014. The importance of large-scale climate variations in modulating flood risks appears to be particularly important in western, central, and southern Africa. Meanwhile, floods in the winter-rain region of South Africa and in East Africa showed weaker teleconnections to large-scale climate variability. Furthermore, while the Pacific and Indian Oceans were found to be the primary drivers of long-term variations in flood occurrence in southern and eastern Africa, the Atlantic Ocean and Mediterranean Sea exhibit a much greater role in western and central Africa. Nevertheless, while these results reveal statistical associations between flooding in SSA and modes of large-scale climate variability, more formal causality testing would help further strengthen our understanding of the causality.

Besides the role of large-scale modes of SSTa, regional circulation patterns may also play a key role in modulating regional and seasonal flood risk. For example, recent studies have shown that the Angola low may weaken or strengthen the effect of ENSO on southern Africa's rainfall (Crétat et al., 2019; Pascale et al., 2019). In addition, while rainfall variability in the winter-rain region of South Africa is known to be primarily related to midlatitude frontal activity in southern Africa (Reason and Rouault, 2005; Dieppois et al., 2016), the weaker large-scale teleconnections observed in this region may also highlight greater influence of human activities on river discharge (Chawanda et al., 2020). Such information is particularly important for developing seamless seasonal and decadal forecasts for flood risk management (Neri et al., 2019; Emerton et al., 2019; Moulds et al., 2023) but were currently missing for the SSA region. They are equally important to further understand how internal climate variability could modulate the effects of anthropogenic climate change and globally rising temperatures on flood risks over the longer-term future (*e.g.,* Deser et al., 2014, 2016; Monerie et al., 2017).

In this regard, based on a statistical framework using 12 CMIP5 and CMIP6 SMILEs, we estimate how different sequences of internal variability, affecting the phasing and amplitude of key climate modes (*e.g.,* ENSO, AMV), could alter the number of floods from one 30-year period to another during the 21st century in 48 sub-catchments in SSA. We find that the future seasonal mean number of floods in SSA could plausibly increase by up to + 10–50 %, or reciprocally decrease by up to −10 to −50 %, relatively to the historical average in response to contrasting sequences of large-scale climate variability from one 30-year period to another over the course of the 21st century. We also note that the relative contributions of large-scale climate variations in modulating future flood risks over the 21st century is regionally consistent across all CMIP5 and CMIP6 SMILEs. Nevertheless, we found slight discrepancies between models, which may be related to contrasting performances in simulating key modes of climate variability, such as ENSO and AMV (McKenna et al., 2020; Richter & Tokinaga, 2020; Coburn & Pryor, 2021). For example, McKenna et al. (2020) demonstrate that certain climate models, such as CSIRO-MK3, GFDL-CM3, and GFDL-ESM2M, tend to overestimate the variance of ENSO and or AMV, and this could lead to greater variations in flood occurrence in these models compare to others in our modelling framework.

Furthermore, our analysis reveals significant positive correlations between the seasonal maximum flood magnitude, duration, and the seasonal number of floods across most stations in SSA, suggesting shared underlying drivers across these flood characteristics. This underscores

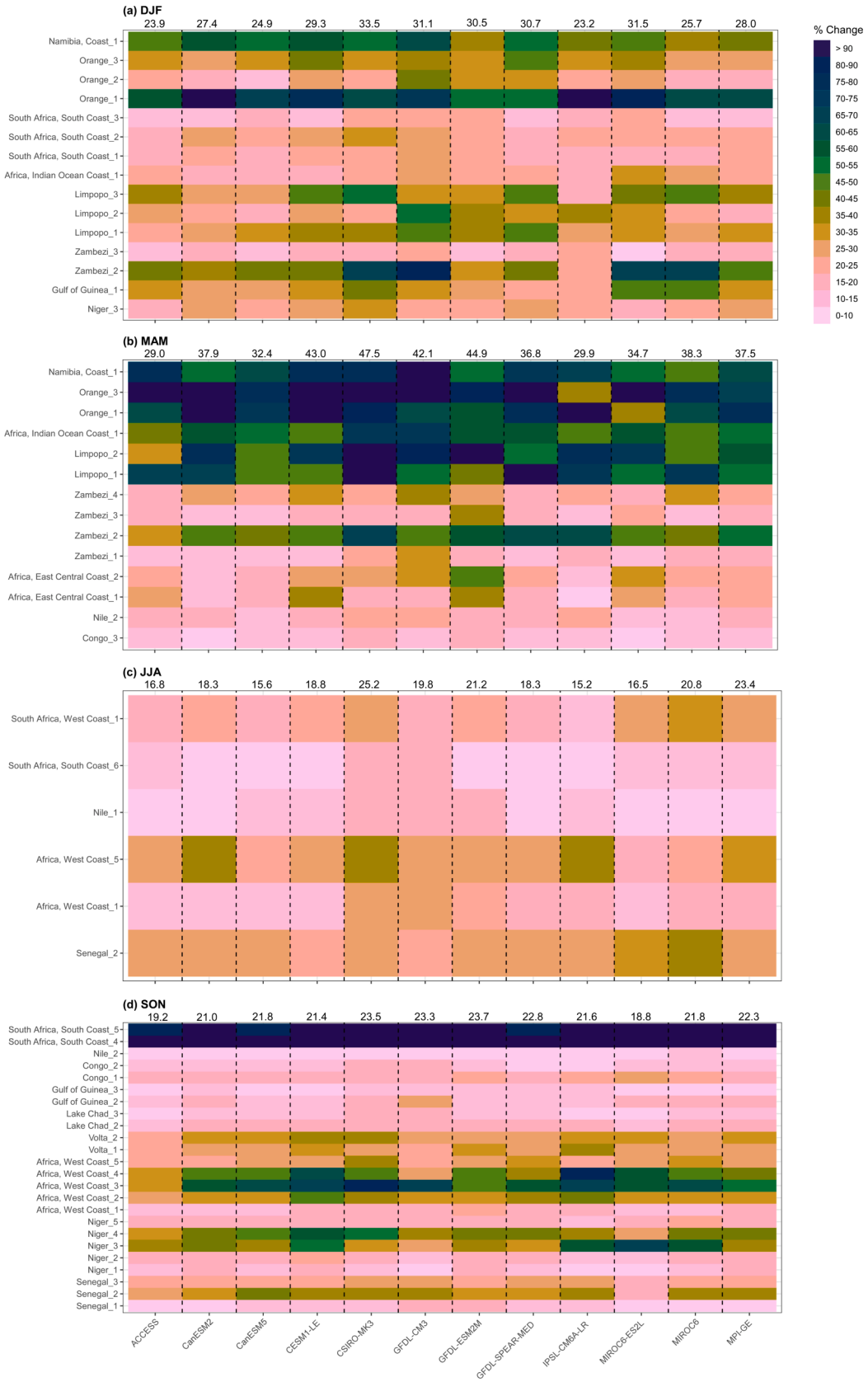

(caption on next page)

Fig. 7. Ensemble spread of the simulated impact of large-scale climate variability on seasonal flood hazards in SSA in each of the CMIP5 and CMIP6 models (1985–2100). a-d) Ensemble standard deviations of the simulated impact of large-scale climate variability on the number of floods occurring in DJF, MAM, JJA and SON across SSA from one 30-year period to another in the 21st century. As for Fig. 6, the impact of large-scale climate variations is estimated using a stepwise generalized linear model with a Poisson distribution. We then calculate the difference between simulated flood frequency over the historical period (1985–2014) and each future 30-year period (SSP-RCP5.85 scenarios: 2015–2100) in 12 CMIP5 and CMIP6 SMILEs (totalling 400 realisations) and estimate the standard deviation for each SMILE. Note that on each panel, only the sub-catchments experiencing at least 30% of their annual total amount of floods during the corresponding seasons are shown.

that internal climate modes of variability may also modulate future changes in flood magnitude and duration in SSA. The extent to which internal climate variability may influence future changes in flood magnitude and duration, however, remain to be quantified and should be the focus of future studies.

By advancing the understanding of potential impacts of climate variability on flooding, our study provides valuable information for effective disaster risk reduction and management. The identification of potential predictors presents a pathway for (a) their inclusion in the design of shorter-term empirical flood risk prediction system, and (b) the development of storylines of long-term combined impacts of internal climate modes of variability and anthropogenic climate changes on flood risks in SSA.

Data and materials availability.

Daily streamflow data are available through the SIEREM (https://www.hydrosciences.fr/sierem/) and the GRDC databases (https://portal.grdc.bafg.de/). CMIP5 and CMIP6 data are publicly available at https://esgf-index1.ceda.ac.uk. ERSST.v5 is available at https://climexp.knmi.nl.

Code availability.

The code used in this study to produce the data analysed was developed in R programming and can be provided upon reasonable request to JE.

funding.

The research leading to these results received funding from the Coventry University Trailblazer PhD studentship scheme, and the Alliance Programme 2021 (Grant No: 814426699), cofounded by the British Council and Campus-France.

CRediT authorship contribution statement

Job Ekolu: Writing – review & editing, Writing – original draft, Visualization, Validation, Supervision, Software, Resources, Project administration, Methodology, Investigation, Formal analysis, Data curation, Conceptualization. **Bastien Dieppois:** Writing – review & editing, Writing – original draft, Visualization, Validation, Supervision, Resources, Project administration, Methodology, Investigation, Funding acquisition, Formal analysis, Data curation, Conceptualization. **Yves Tramblay:** Writing – review & editing, Writing – original draft, Visualization, Validation, Supervision, Methodology, Investigation, Funding acquisition, Formal analysis, Data curation, Conceptualization. **Gabriele Villarini:** Writing – review & editing, Writing – original draft, Visualization, Validation, Methodology, Investigation, Formal analysis, Data curation, Conceptualization. **Louise J. Slater:** Writing – review & editing, Writing – original draft, Visualization, Validation, Methodology, Investigation, Formal analysis, Data curation, Conceptualization. **Gil Mahé:** Writing – review & editing, Writing – original draft, Visualization, Validation, Methodology, Investigation, Formal analysis, Data curation, Conceptualization. **Jean-Emmanuel Paturel:** Writing – review & editing, Writing – original draft, Visualization, Validation, Methodology, Investigation, Formal analysis, Data curation, Conceptualization. **Jonathan M. Eden:** Writing – review & editing, Writing – original draft, Visualization, Validation, Supervision, Methodology, Investigation, Formal analysis, Data curation, Conceptualization. **Simon Moulds:** Writing – review & editing, Writing – original draft, Visualization, Validation, Supervision, Methodology, Investigation, Formal analysis, Data curation, Conceptualization. **Moussa Sidibe:** Writing – review & editing, Writing – original draft, Visualization, Validation, Methodology, Investigation, Formal analysis, Data curation, Conceptualization. **Pierre Camberlin:** Writing – review & editing, Writing – original draft, Visualization, Validation, Methodology, Investigation, Formal analysis, Data curation, Conceptualization. **Benjamin Pohl:** Writing – review & editing, Writing – original draft, Visualization, Validation, Methodology, Investigation, Formal analysis, Data curation, Conceptualization. **Marco van de Wiel:** Writing – review & editing, Writing – original draft, Visualization, Validation, Methodology, Investigation, Formal analysis, Data curation, Conceptualization.

Declaration of competing interest

The authors declare that they have no known competing financial interests or personal relationships that could have appeared to influence the work reported in this paper.

Data availability

The data that has been used is confidential.

Acknowledgments

J.E, B.D, and J.M.E thankfully acknowledge the support from Coventry University, UK, and resources offered by the Centre for Agroecology Water and Resilience (CAWR). In addition, B.D., Y.T, and J.E would like to thank the British Council and Campus-France for their financial support (Alliance Programme 2021; Grant No: 814426699). L. S. is supported by UKRI (MR/V022008/1).

Appendix A. Supplementary data

Supplementary data to this article can be found online at https://doi.org/10.1016/j.jhydrol.2024.131679.

References

Aich, V., Liersch, S., Vetter, T., Fournet, S., Andersson, J.C.M., Calmanti, S., van Weert, F. H.A., Hattermann, F.F., Paton, E.N., 2016. Flood projections within the Niger River Basin under future land use and climate change. Science of the Total Environment 562, 666–677. https://doi.org/10.1016/j.scitotenv.2016.04.021.

Andersson, J.C.M., Ali, A., Arheimer, B., Gustafsson, D., Minoungou, B., 2017. Providing peak river flow statistics and forecasting in the Niger River basin. Physics and Chemistry of the Earth, Parts a/b/c 100, 3–12. https://doi.org/10.1016/j.pce.2017.02.010.

Azen, R., Budescu, D.V., 2003. The dominance analysis approach for comparing predictors in multiple regression. Psychological Methods 8, 129–148. https://doi.org/10.1037/1082-989X.8.2.129.

Azen, R., Traxel, N., 2009. Using Dominance Analysis to Determine Predictor Importance in Logistic Regression. Journal of Educational and Behavioral Statistics 34 (3), 319–347. https://doi.org/10.3102/1076998609332754.

Bates, B.C., Kundzewicz, Z.W., Wu, S., Palutikof , J.P., (Eds.), Climate Change and Water. Technical Paper of the Intergovernmental Panel on Climate Change, IPCC Secretariat, Geneva (2008), p. 210.

Bernard, B., Vincent, K., Frank, M., Anthony, E., 2013. Comparison of extreme weather events and streamflow from drought indices and a hydrological model in River Malaba, Eastern Uganda. International Journal of Environmental Studies 70 (6), 940–951. https://doi.org/10.1080/00207233.2013.862463.

Biasutti, M., Held, I.M., Sobel, A.H., Giannini, A., 2008. SST Forcings and Sahel Rainfall Variability in Simulations of the Twentieth and Twenty-First Centuries. Journal of Climate 21 (14), 3471–3486. https://doi.org/10.1175/2007JCLI1896.1.

Black, E., Slingo, J., Sperber, K.R., 2003. An Observational Study of the Relationship between Excessively Strong Short Rains in Coastal East Africa and Indian Ocean SST. Monthly Weather Review 131 (1), 74–94. https://doi.org/10.1175/1520-0493(2003)131<0074:AOSOTR>2.0.CO;2.

Blume, T., Zehe, E., Bronstert, A., 2007. Rainfall—Runoff response, event-based runoff coefficients and hydrograph separation. Hydrological Sciences Journal 52 (5), 843–862. https://doi.org/10.1623/hysj.52.5.843.

Boucher, O., Servonnat, J., Albright, A. L., Aumont, O., Balkanski, Y., Bastrikov, V., Bekki, S., Bonnet, R., Bony, S., Bopp, L., Braconnot, P., Brockmann, P., Cadule, P., Caubel, A., Cheruy, F., Codron, F., Cozic, A., Cugnet, D., D'Andrea, F., Davini, P., de Lavergne, C., Denvil, S., Deshayes, J., Devilliers, M., Ducharne, A., Dufresne, J.-L., Dupont, E., Éthé, C., Fairhead, L., Falletti, L., Flavoni, S., Foujols, M.-A., Gardoll, S., Gastineau, G., Ghattas, J., Grandpeix, J.-Y., Guenet, B., Guez, Lionel, E., Guilyardi, E., Guimberteau, M., Hauglustaine, D., Hourdin, F., Idelkadi, A., Joussaume, S., Kageyama, M., Khodri, M., Krinner, G., Lebas, N., Levavasseur, G., Lévy, C., Li, L., Lott, F., Lurton, T., Luyssaert, S., Madec, G., Madeleine, J.- B., Maignan, F., Marchand, M., Marti, O., Mellul, L., Meurdesoif, Y., Mignot, J., Musat, I., Ottlé, C., Peylin, P., Planton, Y., Polcher, J., Rio, C., Rochetin, N., Rousset, C., Sepulchre, P., Sima, A., Swingedouw, D., Thiéblemont, R., Traore, A. K., Van-coppenolle, M., Vial, J., Vialard, J., Viovy, N., and Vuichard, N. (2020). Presentation and Evaluation of the IPSL-CM6A-LR Climate Model. Journal of Advances in Modeling Earth Systems, 12(7), e2019MS002010. Doi: 10.1029/2019MS002010.

Boyer, J.F., Dieulin, C., Rouche, N., Cres, A., Servat, E., Paturel, J.E., Mahé, G., 2006. SIEREM: An environmental information system for water resources. Proceedings of IAHS 308, 19–25.

Brunner, M.I., 2021. Reservoir regulation affects droughts and floods at local and regional scales. Environmental Research Letters 16 (12), 124016. https://doi.org/10.1088/1748-9326/ac36f6.

Budescu, D.V., 1993. Dominance analysis: A new approach to the problem of relative importance of predictors in multiple regression. Psychological Bulletin 114 (3), 542–551. https://doi.org/10.1037/0033-2909.114.3.542.

Burger, F.A., Terhaar, J., Frölicher, T.L., 2022. Compound marine heatwaves and ocean acidity extremes. Nature Communications 13 (1), 4722. https://doi.org/10.1038/s41467-022-32120-7.

Cai, W., Ng, B., Wang, G., Santoso, A., Wu, L., Yang, K., 2022. Increased ENSO sea surface temperature variability under four IPCC emission scenarios. Nature Climate Change 12 (3), 228–231. https://doi.org/10.1038/s41558-022-01282-z.

Camberlin, P., 1995. June-september rainfall in north-eastern Africa and atmospheric signals over the tropics: A zonal perspective. International Journal of Climatology 15 (7), 773–783. https://doi.org/10.1002/joc.3370150705.

Camberlin, P., 1997. Rainfall Anomalies in the Source Region of the Nile and Their Connection with the Indian Summer Monsoon. Journal of Climate 10 (6), 1380–1392. https://doi.org/10.1175/1520-0442(1997)010<1380:RAITSR>2.0.CO;2.

Camberlin, P., Okoola, R.E., 2003. The onset and cessation of the "long rains" in eastern Africa and their interannual variability. Theoretical and Applied Climatology 75 (1), 43–54. https://doi.org/10.1007/s00704-002-0721-5.

Casse, C., Gosset, M., Vischel, T., Quantin, G., Tanimoun, B.A., 2016. Model-based study of the role of rainfall and land use–land cover in the changes in the occurrence and intensity of Niger red floods in Niamey between 1953 and 2012. Hydrology and Earth System Sciences 20 (7), 2841–2859. https://doi.org/10.5194/hess-20-2841-2016.

Chapman, T. G., & Maxwell, A. I. (1996). Baseflow separation-comparison of numerical methods with tracer experiments. In Hydrology and water resources symposium 1996: Institution of Engineers, Australia. Water and the environment, 539-545.

Chawanda, C.J., Arnold, J., Thiery, W., van Griensven, A., 2020. Mass balance calibration and reservoir representations for large-scale hydrological impact studies using SWAT+. Climatic Change 163 (3), 1307–1327. https://doi.org/10.1007/s10584-020-02924-x.

Chun, K.P., Dieppois, B., He, Q., Sidibe, M., Eden, J., Paturel, J.-E., Mahé, G., Rouché, N., Klaus, J., Conway, D., 2021. Identifying drivers of streamflow extremes in West Africa to inform a nonstationary prediction model. Weather and Climate Extremes 100346. https://doi.org/10.1016/j.wace.2021.100346.

Coburn, J., Pryor, S.C., 2021. Differential Credibility of Climate Modes in CMIP6. Journal of Climate 34 (20), 8145–8164. https://doi.org/10.1175/JCLI-D-21-0359.1.

Conway, D., 2005. From headwater tributaries to international river: Observing and adapting to climate variability and change in the Nile basin. Global Environmental Change 15 (2), 99–114. https://doi.org/10.1016/j.gloenvcha.2005.01.003.

Conway, D., Persechino, A., Ardoin-Bardin, S., Hamandawana, H., Dieulin, C., Mahé, G., 2009. Rainfall and water resources variability in sub-Saharan Africa during the twentieth century. Journal of Hydrometeorology 10 (1), 41–59.

Crétat, J., Pohl, B., Dieppois, B., Berthou, S., Pergaud, J., 2019. The Angola Low: Relationship with southern African rainfall and ENSO. Climate Dynamics 52 (3), 1783–1803. https://doi.org/10.1007/s00382-018-4222-3.

Dankers, R., Arnell, N.W., Clark, D.B., Falloon, P.D., Fekete, B.M., Gosling, S.N., Heinke, J., Kim, H., Masaki, Y., Satoh, Y., Stacke, T., Wada, Y., Wisser, D., 2014. First look at changes in flood hazard in the Inter-Sectoral Impact Model Intercomparison Project ensemble. Proceedings of the National Academy of Sciences 111 (9), 3257–3261. https://doi.org/10.1073/pnas.1302078110.

Degefu, M.A., Alamirew, T., Zeleke, G., Bewket, W., 2019. Detection of trends in hydrological extremes for Ethiopian watersheds, 1975–2010. Regional Environmental Change 19 (7), 1923–1933. https://doi.org/10.1007/s10113-019-01510-x.

Delworth, T.L., Cooke, W.F., Adcroft, A., Bushuk, M., Chen, J.-H., Dunne, K.A., Ginoux, P., Gudgel, R., Hallberg, R.W., Harris, L., Harrison, M.J., Johnson, N., Kapnick, S.B., Lin, S.-J., Lu, F., Malyshev, S., Milly, P.C., Murakami, H., Naik, V., Pascale, S., Paynter, D., Rosati, A., Schwarzkopf, M., Shevliakova, E., Underwood, S., Wittenberg, A.T., Xiang, B., Yang, X., Zeng, F., Zhang, H., Zhang, L., Zhao, M., 2020. SPEAR: The Next Generation GFDL Modeling System for Seasonal to Multidecadal Prediction and Projection. Journal of Advances in Modeling Earth Systems 12 (3), e2019MS001895. https://doi.org/10.1029/2019MS001895.

Dembélé, M., Vrac, M., Ceperley, N., Zwart, S.J., Larsen, J., Dadson, S.J., Mariéthoz, G., Schaefli, B., 2022. Contrasting changes in hydrological processes of the Volta River basin under global warming. Hydrology and Earth System Sciences 26 (5), 1481–1506. https://doi.org/10.5194/hess-26-1481-2022.

Descroix, L., Moussa, I.B., Genthon, P., Sighomnou, D., Mahé, G., Mamadou, I., Vandervaere, J.-P., Gautier, E., Maiga, O.F., Rajot, J.-L., 2013. Impact of drought and land–use changes on surface–water quality and quantity: The Sahelian paradox. Current Perspectives in Contaminant Hydrology and Water Resources Sustainability 2, 64.

Descroix, L., Guichard, F., Grippa, M., Lambert, L.A., Panthou, G., Mahé, G., Gal, L., Dardel, C., Quantin, G., Kergoat, L., Bouaïta, Y., Hiernaux, P., Vischel, T., Pellarin, T., Faty, B., Wilcox, C., Malam Abdou, M., Mamadou, I., Vandervaere, J.-P., Paturel, J.-E., 2018. Evolution of Surface Hydrology in the Sahelo-Sudanian Strip: An Updated Review. Water 10 (6), Article 6. https://doi.org/10.3390/w10060748.

Deser, C., Phillips, A.S., 2023. A range of outcomes: The combined effects of internal variability and anthropogenic forcing on regional climate trends over Europe. Nonlinear Processes in Geophysics 30 (1), 63–84. https://doi.org/10.5194/npg-30-63-2023.

Deser, C., Phillips, A., Bourdette, V., Teng, H., 2012. Uncertainty in climate change projections: The role of internal variability. Climate Dynamics 38 (3), 527–546. https://doi.org/10.1007/s00382-010-0977-x.

Deser, C., Phillips, A.S., Alexander, M.A., Smoliak, B.V., 2014. Projecting North American Climate over the Next 50 Years: Uncertainty due to Internal Variability. Journal of Climate 27 (6), 2271–2296. https://doi.org/10.1175/JCLI-D-13-00451.1.

Deser, C., Terray, L., Phillips, A.S., 2016. Forced and Internal Components of Winter Air Temperature Trends over North America during the past 50 Years: Mechanisms and Implications. Journal of Climate 29 (6), 2237–2258. https://doi.org/10.1175/JCLI-D-15-0304.1.

Dieppois, B., Diedhiou, A., Durand, A., Fournier, M., Massei, N., Sebag, D., Xue, Y., Fontaine, B., 2013. Quasi-decadal signals of Sahel rainfall and West African monsoon since the mid-twentieth century. Journal of Geophysical Research: Atmospheres 118 (22), 12–587.

Dieppois, B., Pohl, B., Rouault, M., New, M., Lawler, D., Keenlyside, N., 2016. Interannual to interdecadal variability of winter and summer southern African rainfall, and their teleconnections. Journal of Geophysical Research: Atmospheres 121 (11), 6215–6239. https://doi.org/10.1002/2015JD024576.

Dieppois, B., Durand, A., Fournier, M., Diedhiou, A., Fontaine, B., Massei, N., Nouaceur, Z., Sebag, D., 2015. Low-frequency variability and zonal contrast in Sahel rainfall and Atlantic sea surface temperature teleconnections during the last century. Theoretical and Applied Climatology 121 (1), 139–155. https://doi.org/10.1007/s00704-014-1229-5.

Dieppois, B., Pohl, B., Crétat, J., Eden, J., Sidibe, M., New, M., Rouault, M., Lawler, D., 2019. Southern African summer-rainfall variability, and its teleconnections, on interannual to interdecadal timescales in CMIP5 models. Climate Dynamics 53, 3505–3527. https://doi.org/10.1007/s00382-019-04720-5.

Dieppois, B., Capotondi, A., Pohl, B., Chun, K.P., Monerie, P.-A., Eden, J., 2021. ENSO diversity shows robust decadal variations that must be captured for accurate future projections. Communications Earth & Environment 2 (1), Article 1. https://doi.org/10.1038/s43247-021-00285-6.

Dixon, H., Sandström, S., Cudennec, C., Lins, H.F., Abrate, T., Bérod, D., Chernov, I., Ravalitera, N., Sighomnou, D., Teichert, F., 2022. Intergovernmental cooperation for hydrometry – what, why and how? Hydrological Sciences Journal 67 (16), 2552–2566. https://doi.org/10.1080/02626667.2020.1764569.

Do, H.X., Westra, S., Leonard, M., 2017. A global-scale investigation of trends in annual maximum streamflow. Journal of Hydrology 552, 28–43. https://doi.org/10.1016/j.jhydrol.2017.06.015.

Dunning, C.M., Black, E.C.L., Allan, R.P., 2016. The onset and cessation of seasonal rainfall over Africa. Journal of Geophysical Research: Atmospheres 121 (19), 11405–11424. https://doi.org/10.1002/2016JD025428.

Ekolu, J., Dieppois, B., Sidibe, M., Eden, J.M., Tramblay, Y., Villarini, G., Peña-Angulo, D., Mahé, G., Paturel, J.-E., Onyutha, C., van de Wiel, M., 2022. Long-term variability in hydrological droughts and floods in sub-Saharan Africa: New perspectives from a 65-year daily streamflow dataset. Journal of Hydrology 613, 128359. https://doi.org/10.1016/j.jhydrol.2022.128359.

Emerton, R.E., Stephens, E.M., Cloke, H.L., 2019. What is the most useful approach for forecasting hydrological extremes during El Niño? Environmental Research Communications 1 (3), 031002. https://doi.org/10.1088/2515-7620/ab114e.

Enfield, D.B., Mestas-Nuñez, A.M., Mayer, D.A., Cid-Serrano, L., 1999. How ubiquitous is the dipole relationship in tropical Atlantic sea surface temperatures? Journal of Geophysical Research: Oceans 104 (C4), 7841–7848. https://doi.org/10.1029/1998JC900109.

Enfield, D.B., Mestas-Nuñez, A.M., Trimble, P.J., 2001. The Atlantic Multidecadal Oscillation and its relation to rainfall and river flows in the continental U.S. Geophysical Research Letters 28 (10), 2077–2080. https://doi.org/10.1029/2000GL0127458<1069:APICOW>2.0.CO;2.

Fasullo, J.T., Phillips, A.S., Deser, C., 2020. Evaluation of Leading Modes of Climate Variability in the CMIP Archives. Journal of Climate 33 (13), 5527–5545. https://doi.org/10.1175/JCLI-D-19-1024.1.

Ficchì, A., Stephens, L., 2019. Climate Variability Alters Flood Timing Across Africa. Geophysical Research Letters 46 (15), 8809–8819. https://doi.org/10.1029/2019GL081988.

Ficchì, A., Cloke, H., Neves, C., Woolnough, S., Coughlan de Perez, E., Zsoter, E., Pinto, I., Meque, A., Stephens, E., 2021. Beyond El Niño: Unsung climate modes drive African

floods. Weather and Climate Extremes 33, 100345. https://doi.org/10.1016/j.wace.2021.100345.
Fontaine, B., Garcia-Serrano, J., Roucou, P., Rodriguez-Fonseca, B., Losada, T., Chauvin, F., Gervois, S., Sijikumar, S., Ruti, P., Janicot, S., 2010. Impacts of warm and cold situations in the Mediterranean basins on the West African monsoon: Observed connection patterns (1979–2006) and climate simulations. Climate Dynamics 35 (1), 95–114. https://doi.org/10.1007/s00382-009-0599-3.
Fontaine, B., Monerie, P.-A., Gaetani, M., Roucou, P., 2011. Climate adjustments over the African-Indian monsoon regions accompanying Mediterranean Sea thermal variability. Journal of Geophysical Research: Atmospheres 116 (D23). https://doi.org/10.1029/2011JD016273.
Franchi, F., Mustafa, S., Ariztegui, D., Chirindja, F.J., Di Capua, A., Hussey, S., Loizeau, J.-L., Maselli, V., Matanó, A., Olabode, O., Pasqualotto, F., Sengwei, W., Tirivarombo, S., Van Loon, A.F., Comte, J.-C., 2024. Prolonged drought periods over the last four decades increase flood intensity in southern Africa. Science of the Total Environment 924, 171489. https://doi.org/10.1016/j.scitotenv.2024.171489.
Gaetani, M., Fontaine, B., Roucou, P., Baldi, M., 2010. Influence of the Mediterranean Sea on the West African monsoon: Intraseasonal variability in numerical simulations. Journal of Geophysical Research: Atmospheres 115 (D24). https://doi.org/10.1029/2010JD014436.
Giannini, A., Saravanan, R., Chang, P., 2005. Dynamics of the boreal summer African monsoon in the NSIPP1 atmospheric model. Climate Dynamics 25 (5), 517–535. https://doi.org/10.1007/s00382-005-0056-x.
Giannini, A., Biasutti, M., Held, I.M., Sobel, A.H., 2008. A global perspective on African climate. Climatic Change 90 (4), 359–383. https://doi.org/10.1007/s10584-008-9396-y.
Gosling, S.N., Arnell, N.W., 2016. A global assessment of the impact of climate change on water scarcity. Climatic Change 134 (3), 371–385. https://doi.org/10.1007/s10584-013-0853-x.
Hajima, T., Watanabe, M., Yamamoto, A., Tatebe, H., Noguchi, M.A., Abe, M., Ohgaito, R., Ito, A., Yamazaki, D., Okajima, H., Ito, A., Takata, K., Ogochi, K., Watanabe, S., Kawamiya, M., 2020. Development of the MIROC-ES2L Earth system model and the evaluation of biogeochemical processes and feedbacks. Geoscientific Model Development 13 (5), 2197–2244. https://doi.org/10.5194/gmd-13-2197-2020.
Harrigan, S., Zsoter, E., Alfieri, L., Prudhomme, C., Salamon, P., Wetterhall, F., Barnard, C., Cloke, H., Pappenberger, F., 2020. GloFAS-ERA5 operational global river discharge reanalysis 1979–present. Earth System Science Data 12 (3), 2043–2060. https://doi.org/10.5194/essd-12-2043-2020.
Henley, B.J., Gergis, J., Karoly, D.J., Power, S., Kennedy, J., Folland, C.K., 2015. A Tripole Index for the Interdecadal Pacific Oscillation. Climate Dynamics 45 (11), 3077–3090. https://doi.org/10.1007/s00382-015-2525-1.
Hirabayashi, Y., Mahendran, R., Koirala, S., Konoshima, L., Yamazaki, D., Watanabe, S., Kim, H., Kanae, S., 2013. Global flood risk under climate change. Nature Climate Change 3 (9), 816–821. https://doi.org/10.1038/nclimate1911.
Hoell, A., Cheng, L., 2018. Austral summer Southern Africa precipitation extremes forced by the El Niño-Southern oscillation and the subtropical Indian Ocean dipole. Climate Dynamics 50 (9), 3219–3236. https://doi.org/10.1007/s00382-017-3801-z.
Hoell, A., Funk, C., Magadzire, T., Zinke, J., Husak, G., 2015. El Niño-Southern Oscillation diversity and Southern Africa teleconnections during Austral Summer. Climate Dynamics 45 (5), 1583–1599. https://doi.org/10.1007/s00382-014-2414-z.
Huang, S., Li, P., Huang, Q., Leng, G., Hou, B., Ma, L., 2017. The propagation from meteorological to hydrological drought and its potential influence factors. Journal of Hydrology 547, 184–195. https://doi.org/10.1016/j.jhydrol.2017.01.041.
Jain, S., Scaife, A.A., Shepherd, T.G., Deser, C., Dunstone, N., Schmidt, G.A., Trenberth, K.E., Turkington, T., 2023. Importance of internal variability for climate model assessment. Npj Climate and Atmospheric Science 6, 68. https://doi.org/10.1038/s41612-023-00389-0.
Janowiak, J.E., 1988. An Investigation of Interannual Rainfall Variability in Africa. Journal of Climate 1 (3), 240–255. https://doi.org/10.1175/1520-0442(1988)001<0240:AIOIRV>2.0.CO;2.
Jeffrey, S., Rotstayn, L., Collier, M., Dravitzki, S., Hamalainen, C., Moeseneder, C., Wong, K., Syktus, J., 2013. Australia's CMIP5 submission usingthe CSIRO-Mk3.6 model. Australian Meteorological and Oceanographic Journal 63 (1), 1–13. https://doi.org/10.1071/es13001.
Kay, J.E., Deser, C., Phillips, A., Mai, A., Hannay, C., Strand, G., Arblaster, J.M., Bates, S. C., Danabasoglu, G., Edwards, J., Holland, M., Kushner, P., Lamarque, J.-F., Lawrence, D., Lindsay, K., Middleton, A., Munoz, E., Neale, R., Oleson, K., Vertenstein, M., 2015. The Community Earth System Model (CESM) Large Ensemble Project: A Community Resource for Studying Climate Change in the Presence of Internal Climate Variability. Bulletin of the American Meteorological Society 96 (8), 1333–1349. https://doi.org/10.1175/BAMS-D-13-00255.1.
Kingston, D.G., Massei, N., Dieppois, B., Hannah, D.M., Hartmann, A., Lavers, D.A., Vidal, J.-P., 2020. Moving beyond the catchment scale: Value and opportunities in large-scale hydrology to understand our changing world. Hydrological Processes 34 (10), 2292–2298.
Kirchmeier-Young, M.C., Zwiers, F.W., Gillett, N.P., 2017. Attribution of Extreme Events in Arctic Sea Ice Extent. Journal of Climate 30 (2), 553–571. https://doi.org/10.1175/JCLI-D-16-0412.1.
Kundzewicz, Z.W., Szwed, M., Pińskwar, I., 2019. Climate variability and floods—A global review. Water 11 (7), 1399.
Leggesse, E.S., Beyene, B.S., 2017. Hydrology of Lake Tana Basin. In: Stave, K., Goshu, G., Aynalem, S. (Eds.), Social and Ecological System Dynamics: Characteristics, Trends, and Integration in the Lake Tana Basin, Ethiopia. Springer International Publishing, pp. 117–126. https://doi.org/10.1007/978-3-319-45755-0_9.
Lehner, F., Deser, C., Maher, N., Marotzke, J., Fischer, E.M., Brunner, L., Knutti, R., Hawkins, E., 2020. Partitioning climate projection uncertainty with multiple large ensembles and CMIP5/6. Earth System Dynamics 11 (2), 491–508. https://doi.org/10.5194/esd-11-491-2020.
Liebmann, B., Bladé, I., Kiladis, G.N., Carvalho, L.M.V., Senay, G.B., Allured, D., Leroux, S., Funk, C., 2012. Seasonality of African Precipitation from 1996 to 2009. Journal of Climate 25 (12), 4304–4322. https://doi.org/10.1175/JCLI-D-11-00157.1.
Losada, T., Rodríguez-Fonseca, B., Janicot, S., Gervois, S., Chauvin, F., Ruti, P., 2010. A multi-model approach to the Atlantic Equatorial mode: Impact on the West African monsoon. Climate Dynamics 35 (1), 29–43. https://doi.org/10.1007/s00382-009-0625-5.
Luo, W., Azen, R., 2013. Determining Predictor Importance in Hierarchical Linear Models Using Dominance Analysis. Journal of Educational and Behavioral Statistics 38 (1), 3–31. https://doi.org/10.3102/1076998612458319.
Lyon, B., Mason, S.J., 2007. The 1997–98 Summer Rainfall Season in Southern Africa. Part i: Observations. Journal of Climate 20 (20), 5134–5148. https://doi.org/10.1175/JCLI4225.1.
Mahe, G., Lienou, G., Descroix, L., Bamba, F., Paturel, J.E., Laraque, A., Meddi, M., Habaieb, H., Adeaga, O., Dieulin, C., Kotti, F.C., Khomsi, K., 2013. The rivers of Africa: Witness of climate change and human impact on the environment. Hydrological Processes 27 (15), 2105–2114. https://doi.org/10.1002/hyp.9813.
Maher, N., Milinski, S., Suarez-Gutierrez, L., Botzet, M., Dobrynin, M., Kornblueh, L., Kröger, J., Takano, Y., Ghosh, R., Hedemann, C., Li, C., Li, H., Manzini, E., Notz, D., Putrasahan, D., Boysen, L., Claussen, M., Ilyina, T., Olonscheck, D., Marotzke, J., 2019. The Max Planck Institute Grand Ensemble: Enabling the Exploration of Climate System Variability. Journal of Advances in Modeling Earth Systems 11 (7), 2050–2069. https://doi.org/10.1029/2019MS001639.
Maher, N., Milinski, S., Ludwig, R., 2021. Large ensemble climate model simulations: Introduction, overview, and future prospects for utilising multiple types of large ensemble. Earth System Dynamics 12 (2), 401–418. https://doi.org/10.5194/esd-12-401-2021.
Maher, N., Wills, R.C.J., DiNezio, P., Klavans, J., Milinski, S., Sanchez, S.C., Stevenson, S., Stuecker, M.F., Wu, X., 2023. The future of the El Niño-Southern Oscillation: Using large ensembles to illuminate time-varying responses and inter-model differences. Earth System Dynamics 14 (2), 413–431. https://doi.org/10.5194/esd-14-413-2023.
Manatsa, D., Behera, S.K., 2013. On the Epochal Strengthening in the Relationship between Rainfall of East Africa and IOD. Journal of Climate 26 (15), 5655–5673. https://doi.org/10.1175/JCLI-D-12-00568.1.
Manatsa, D., Reason, C.J.C., Mukwada, G., 2012. On the decoupling of the IODZM from southern Africa Summer rainfall variability. International Journal of Climatology 32 (5), 727–746. https://doi.org/10.1002/joc.2306.
Mangini, W., Viglione, A., Hall, J., Hundecha, Y., Ceola, S., Montanari, A., Rogger, M., Salinas, J.L., Borzì, I., Parajka, J., 2018. Detection of trends in magnitude and frequency of flood peaks across Europe. Hydrological Sciences Journal 63 (4), 493–512. https://doi.org/10.1080/02626667.2018.1444766.
Mantua, N.J., Hare, S.R., Zhang, Y., Wallace, J.M., Francis, R.C., 1997. A Pacific Interdecadal Climate Oscillation with Impacts on Salmon Production*. Bulletin of the American Meteorological Society 78 (6), 1069–1080. https://doi.org/10.1175/1520-0477(1997)07.
McKenna, S., Santoso, A., Gupta, A.S., Taschetto, A.S., Cai, W., 2020. Indian Ocean Dipole in CMIP5 and CMIP6: Characteristics, biases, and links to ENSO. Scientific Reports 10, 11500. https://doi.org/10.1038/s41598-020-68268-9.
Mei, Y., Anagnostou, E.N., 2015. A hydrograph separation method based on information from rainfall and runoff records. Journal of Hydrology 523, 636–649. https://doi.org/10.1016/j.jhydrol.2015.01.083.
Milinski, S., Maher, N., Olonscheck, D., 2020. How large does a large ensemble need to be? Earth System Dynamics 11 (4), 885–901. https://doi.org/10.5194/esd-11-885-2020.
Mohino, E., Janicot, S., Bader, J., 2011. Sahel rainfall and decadal to multi-decadal sea surface temperature variability. Climate Dynamics 37 (3), 419–440. https://doi.org/10.1007/s00382-010-0867-2.
Monerie, P.-A., Sanchez-Gomez, E., Pohl, B., Robson, J., Dong, B., 2017. Impact of internal variability on projections of Sahel precipitation change. Environmental Research Letters 12 (11), 114003.
Monerie, P.-A., Robson, J., Dong, B., Dieppois, B., Pohl, B., Dunstone, N., 2019. Predicting the seasonal evolution of southern African summer precipitation in the DePreSys3 prediction system. Climate Dynamics 52 (11), 6491–6510. https://doi.org/10.1007/s00382-018-4526-3.
Moulds, S., Slater, L.J., Dunstone, N.J., Smith, D.M., 2023. Skillful Decadal Flood Prediction. Geophysical Research Letters 50 (3), e2022GL100650. https://doi.org/10.1029/2022GL100650.
Mutai, C.C., Ward, M.N., Colman, A.W., 1998. Towards the prediction of the East Africa short rains based on sea-surface temperature–atmosphere coupling. International Journal of Climatology 18 (9), 975–997. https://doi.org/10.1002/(SICI)1097-0088(199807)18:9<975::AID-JOC259>3.0.CO;2-U.
Nathan, R.J., McMahon, T.A., 1990. Evaluation of automated techniques for base flow and recession analyses. Water Resources Research 26 (7), 1465–1473. https://doi.org/10.1029/WR026i007p01465.
Neri, A., Villarini, G., Salvi, K.A., Slater, L.J., Napolitano, F., 2019. On the decadal predictability of the frequency of flood events across the U.S. Midwest. International Journal of Climatology 39 (3), 1796–1804. https://doi.org/10.1002/joc.5915.
Niang, I., Ruppel, O.C., Abdrabo, M.A., Essel, A., Lennard, C., Padgham, J. and Urquhart, P. (2014) Africa. In: Barros, V.R., Field, C.B., Dokken, D.J., Mastrandrea, M.D., Mach, K.J., Bilir, T.E., Chatterjee, M., Ebi, K.L., Estrada, Y.O., Genova, R.C., Girma,

B., Kissel, E.S., Levy, A.N., MacCracken, S., Mastrandrea, P.R. and White, L.L., Eds., Climate Change 2014: Impacts, Adaptation, and Vulnerability. Part B: Regional Aspects. Contribution of Working Group II to the Fifth Assessment Report of the Intergovernmental Panel on Climate Change, Cambridge University Press, Cambridge, 1199-1265.

Nicholson, S.E., 2017. Climate and climatic variability of rainfall over eastern Africa. Reviews of Geophysics 55 (3), 590–635. https://doi.org/10.1002/2016RG000544.

Nicholson, S., e., & Selato, J. c, 2000. The influence of La Nina on African rainfall. International Journal of Climatology 20 (14), 1761–1776. https://doi.org/10.1002/1097-0088(20001130)20:14<1761::AID-JOC580>3.0.CO;2-W.

Nka, B.N., Oudin, L., Karambiri, H., Paturel, J.-E., Ribstein, P., 2015. Trends in floods in West Africa: Analysis based on 11 catchments in the region. Hydrology and Earth System Sciences 19 (11), 4707–4719.

Nobre, G.G., Jongman, B., Aerts, J., Ward, P.J., 2017. The role of climate variability in extreme floods in Europe. Environmental Research Letters 12 (8), 084012. https://doi.org/10.1088/1748-9326/aa7c22.

Nyeko-Ogiramoi, P., Willems, P., Ngirane-Katashaya, G., 2013. Trend and variability in observed hydrometeorological extremes in the Lake Victoria basin. Journal of Hydrology 489, 56–73. https://doi.org/10.1016/j.jhydrol.2013.02.039.

Ogallo, L.J., 1988. Relationships between seasonal rainfall in East Africa and the Southern Oscillation. Journal of Climatology 8 (1), 31–43. https://doi.org/10.1002/joc.3370080104.

Omondi, P., Ogallo, L.A., Anyah, R., Muthama, J.M., Ininda, J., 2013. Linkages between global sea surface temperatures and decadal rainfall variability over Eastern Africa region. International Journal of Climatology 33 (8), 2082–2104. https://doi.org/10.1002/joc.3578.

Parhi, P., Giannini, A., Gentine, P., Lall, U., 2016. Resolving Contrasting Regional Rainfall Responses to El Niño over Tropical Africa. Journal of Climate 29 (4), 1461–1476. https://doi.org/10.1175/JCLI-D-15-0071.1.

Pascale, S., Pohl, B., Kapnick, S.B., Zhang, H., 2019. On the Angola Low Interannual Variability and Its Role in Modulating ENSO Effects in Southern Africa. Journal of Climate 32 (15), 4783–4803. https://doi.org/10.1175/JCLI-D-18-0745.1.

Philippon, N., Rouault, M., Richard, Y., Favre, A., 2012. The influence of ENSO on winter rainfall in South Africa. International Journal of Climatology 32 (15), 2333–2347. https://doi.org/10.1002/joc.3403.

Pohl, B., Dieppois, B., Crétat, J., Lawler, D., Rouault, M., 2018. From Synoptic to Interdecadal Variability in Southern African Rainfall: Toward a Unified View across Time Scales. Journal of Climate 31 (15), 5845–5872. https://doi.org/10.1175/JCLI-D-17-0405.1.

Rameshwaran, P., Bell, V.A., Davies, H.N., Kay, A.L., 2021. How might climate change affect river flows across West Africa? Climatic Change 169 (3), 21. https://doi.org/10.1007/s10584-021-03256-0.

Rasmusson, E.M., Carpenter, T.H., 1982. Variations in Tropical Sea Surface Temperature and Surface Wind Fields Associated with the Southern Oscillation/El Niño. Monthly Weather Review 110 (5), 354–384. https://doi.org/10.1175/1520-0493(1982)110<0354:VITSST>2.0.CO;2.

Reason, C.J.C., Rouault, M., 2005. Links between the Antarctic Oscillation and winter rainfall over western South Africa. Geophysical Research Letters 32 (7). https://doi.org/10.1029/2005GL022419.

Reason, C., j. c., Allan, R. j., Lindesay, J. a., & Ansell, T. j, 2000. ENSO and climatic signals across the Indian Ocean Basin in the global context: Part I, interannual composite patterns. International Journal of Climatology 20 (11), 1285–1327. https://doi.org/10.1002/1097-0088(200009)20:11<1285::AID-JOC536>3.0.CO;2-R.

Reynolds, R.W., Rayner, N.A., Smith, T.M., Stokes, D.C., Wang, W., 2002. An Improved In Situ and Satellite SST Analysis for Climate. Journal of Climate 15 (13), 1609–1625. https://doi.org/10.1175/1520-0442(2002)015<1609:AIISAS>2.0.CO;2.

Richter, I., Tokinaga, H., 2020. An overview of the performance of CMIP6 models in the tropical Atlantic: Mean state, variability, and remote impacts. Climate Dynamics 55 (9), 2579–2601. https://doi.org/10.1007/s00382-020-05409-w.

Rodríguez-Fonseca, B., Mohino, E., Mechoso, C.R., Caminade, C., Biasutti, M., Gaetani, M., Garcia-Serrano, J., Vizy, E.K., Cook, K., Xue, Y., 2015. Variability and predictability of West African droughts: A review on the role of sea surface temperature anomalies. Journal of Climate 28 (10), 4034–4060.

Roffe, S.J., Fitchett, J.M., Curtis, C.J., 2019. Classifying and mapping rainfall seasonality in South Africa: A review. South African Geographical Journal 101 (2), 158–174. https://doi.org/10.1080/03736245.2019.1573151.

Rowell, D.P., 2013. Simulating SST Teleconnections to Africa: What is the State of the Art? Journal of Climate 26 (15), 5397–5418. https://doi.org/10.1175/JCLI-D-12-00761.1.

Saji, N. H., Goswami, B. N., Vinayachandran, P. N., & Yamagata, T. (1999). A dipole mode in the tropical Indian Ocean. Nature, 401(6751), Article 6751. Doi: 10.1038/43854.

Sauerbrei, W., Schumacher, M., 1992. A bootstrap resampling procedure for model building: Application to the Cox regression model. Statistics in Medicine 11 (16), 2093–2109. https://doi.org/10.1002/sim.4780111607.

Segele, Z.T., Lamb, P.J., Leslie, L.M., 2009. Seasonal-to-Interannual Variability of Ethiopia/Horn of Africa Monsoon. Part I: Associations of Wavelet-Filtered Large-Scale Atmospheric Circulation and Global Sea Surface Temperature. Journal of Climate 22 (12), 3396–3421. https://doi.org/10.1175/2008JCLI2859.1.

Shiferaw, B., Tesfaye, K., Kassie, M., Abate, T., Prasanna, B.M., Menkir, A., 2014. Managing vulnerability to drought and enhancing livelihood resilience in sub-Saharan Africa: Technological, institutional and policy options. Weather and Climate Extremes 3, 67–79. https://doi.org/10.1016/j.wace.2014.04.004.

Sidibe, M., Dieppois, B., Eden, J., Mahé, G., Paturel, J.-E., Amoussou, E., Anifowose, B., Lawler, D., 2019. Interannual to Multi-decadal streamflow variability in West and Central Africa: Interactions with catchment properties and large-scale climate variability. Global and Planetary Change 177, 141–156. https://doi.org/10.1016/j.gloplacha.2019.04.003.

Smith, G., 2018. Step away from stepwise. Journal of Big Data 5 (1), 32. https://doi.org/10.1186/s40537-018-0143-6.

Suarez-Gutierrez, L., Milinski, S., Maher, N., 2021. Exploiting large ensembles for a better yet simpler climate model evaluation. Climate Dynamics 57 (9), 2557–2580. https://doi.org/10.1007/s00382-021-05821-w.

Sun, L., Alexander, M., Deser, C., 2018. Evolution of the Global Coupled Climate Response to Arctic Sea Ice Loss during 1990–2090 and Its Contribution to Climate Change. Journal of Climate 31 (19), 7823–7843. https://doi.org/10.1175/JCLI-D-18-0134.1.

Swart, N. C., Cole, J. N. S., Kharin, V. V., Lazare, M., Scinocca, J. F., Gillett, N. P., Anstey, J., Arora, V., Christian, J. R., Hanna, S., Jiao, Y., Lee, W. G., Majaess, F., Saenko, O. A., Seiler, C., Seinen, C., Shao, A., Sigmond, M., Solheim, L., … Winter, B. (2019). The Canadian Earth System Model version 5 (CanESM5.0.3). Geoscientific Model Development, 12(11), Article 11. https://doi.org/10.5194/gmd-12-4823-2019.

Takahashi, K., Montecinos, A., Goubanova, K., Dewitte, B., 2011. ENSO regimes: Reinterpreting the canonical and Modoki El Niño. Geophysical Research Letters 38 (10). https://doi.org/10.1029/2011GL047364.

Tallaksen, L.M., 1995. A review of baseflow recession analysis. Journal of Hydrology 165 (1), 349–370. https://doi.org/10.1016/0022-1694(94)02540-R.

Tatebe, H., Ogura, T., Nitta, T., Komuro, Y., Ogochi, K., Takemura, T., Sudo, K., Sekiguchi, M., Abe, M., Saito, F., Chikira, M., Watanabe, S., Mori, M., Hirota, N., Kawatani, Y., Mochizuki, T., Yoshimura, K., Takata, K., O'ishi, R., Yamazaki, D., Suzuki, T., Kurogi, M., Kataoka, T., Watanabe, M., and Kimoto, M, 2019. Description and basic evaluation of simulated mean state, internal variability, and climate sensitivity in MIROC6. Geoscientific Model Development 12 (7), 2727–2765. https://doi.org/10.5194/gmd-12-2727-2019.

Taye, M. T., Willems, P., & Block, P. (2015). Implications of climate change on hydrological extremes in the Blue Nile basin: a review. Journal of Hydrology: Regional Studies, 4, 280-293Thomas, B. F., Vogel, R. M., Kroll, C. N., & Famiglietti, J. S. (2013). Estimation of the base flow recession constant under human interference. Water Resources Research, 49(11), Article 11. https://doi.org/10.1002/wrcr.20532.

Taye, M.T., Willems, P., 2012. Temporal variability of hydroclimatic extremes in the Blue Nile basin. Water Resources Research 48 (3). https://doi.org/10.1029/2011WR011466.

Thomas, B. F., Vogel, R. M., Kroll, C. N., & Famiglietti, J. S. (2013). Estimation of the base flow recession constant under human interference. Water Resources Research, 49(11), Article 11. https://doi.org/10.1002/wrcr.20532.

Thorncroft, C.D., Nguyen, H., Zhang, C., Peyrillé, P., 2011. Annual cycle of the West African monsoon: Regional circulations and associated water vapour transport. Quarterly Journal of the Royal Meteorological Society 137 (654), 129–147. https://doi.org/10.1002/qj.728.

Tramblay, Y., Rouché, N., Paturel, J.-E., Mahé, G., Boyer, J.-F., Amoussou, E., Bodian, A., Dacosta, H., Dakhlaoui, H., Dezetter, A., Hughes, D., Hanich, L., Peugeot, C., Tshimanga, R., Lachassagne, P., 2020a. The African Database of Hydrometric Indices (ADHI). Earth System Science Data 13, 1547–1560. https://doi.org/10.5194/essd-13-1547-2021, 2021.

Tramblay, Y., Villarini, G., Zhang, W., 2020b. Observed changes in flood hazard in Africa. Environmental Research Letters 15 (10), 1040b5. https://doi.org/10.1088/1748-9326/abb90b.

Trenberth, K.E., Shea, D.J., 2006. Atlantic hurricanes and natural variability in 2005. Geophysical Research Letters 33 (12). https://doi.org/10.1029/2006GL026894.

Tyson, P.D., Preston-Whyte, R.A., Preston-Whyte, R.A., 2000. Weather and climate of southern Africa. Oxford University Press, p. 396 pp..

Ullah, A., Pohl, B., Pergaud, J., Dieppois, B., Rouault, M., 2022. Intraseasonal descriptors and extremes in South African rainfall. Part I: Summer climatology and statistical characteristics. International Journal of Climatology 42 (9), 4538–4563. https://doi.org/10.1002/joc.7489http://vital.seals.ac.za:8080/vital/access/manager/Repository/vital:6030?site_name=GlobalView.

Vaittinada Ayar, P., Vrac, M., Mailhot, A., 2021. Ensemble bias correction of climate simulations: Preserving internal variability. Scientific Reports 11 (1), Article 1. https://doi.org/10.1038/s41598-021-82715-1.

Valimba, P., 2005. Rainfall variability in Southern Africa, its influences on streamflow variations and its relationships with climatic variations. Rhodes University grahamstown South Africa. Published PhD thesis.

Vizy, E.K., Cook, K.H., 2018. Mesoscale convective systems and nocturnal rainfall over the West African Sahel: Role of the Inter-tropical front. Climate Dynamics 50 (1), 587–614. https://doi.org/10.1007/s00382-017-3628-7.

Vogel, R.M., Kroll, C.N., 1996. Estimation of baseflow recession constants. Water Resources Management 10 (4), 303–320. https://doi.org/10.1007/BF00508898.

Washington, R., Preston, A., 2006. Extreme wet years over southern Africa: Role of Indian Ocean Sea surface temperatures. Journal of Geophysical Research: Atmospheres 111 (D15). https://doi.org/10.1029/2005JD006724.

Webster, P. J., Moore, A. M., Loschnigg, J. P., & Leben, R. R. (1999). Coupled ocean–atmosphere dynamics in the Indian Ocean during 1997–98. Nature, 401(6751), Article 6751. Doi: 10.1038/43848.

Wilcox, C., Vischel, T., Panthou, G., Bodian, A., Blanchet, J., Descroix, L., Quantin, G., Cassé, C., Tanimoun, B., Kone, S., 2018. Trends in hydrological extremes in the Senegal and Niger Rivers. Journal of Hydrology 566, 531–545. https://doi.org/10.1016/j.jhydrol.2018.07.063.

Williams, A.P., Funk, C., Michaelsen, J., Rauscher, S.A., Robertson, I., Wils, T.H.G., Koprowski, M., Eshetu, Z., Loader, N.J., 2012. Recent summer precipitation trends in the Greater Horn of Africa and the emerging role of Indian Ocean sea surface temperature. Climate Dynamics 39 (9), 2307–2328. https://doi.org/10.1007/s00382-011-1222-y.

Winsemius, H.C., Aerts, J.C.J.H., van Beek, L.P.H., Bierkens, M.F.P., Bouwman, A., Jongman, B., Kwadijk, J.C.J., Ligtvoet, W., Lucas, P.L., van Vuuren, D.P., Ward, P.J., 2016. Global drivers of future river flood risk. Nature Climate Change 6 (4), 381–385. https://doi.org/10.1038/nclimate2893.

WMO, (2009). Guide to hydrological practices volume II: management of water resources and application of hydrological practices. Geneva: World Meteorological Organization, WMO Report No 168.

Ziehn, T., Chamberlain, M.A., Law, R.M., Lenton, A., Bodman, R.W., Dix, M., Stevens, L., Wang, Y.-P., Srbinovsky, J., Ziehn, T., Chamberlain, M.A., Law, R.M., Lenton, A., Bodman, R.W., Dix, M., Stevens, L., Wang, Y.-P., Srbinovsky, J.T., System, A.E., Model: ACCESS-ESM1.5, 2020. Journal of Southern Hemisphere Earth Systems Science 70 (1), 193–214. https://doi.org/10.1071/ES19035.